European Journal of Cell Biology 94 (2015) 626–641

Contents lists available at ScienceDirect

European Journal of Cell Biology

journal homepage: www.elsevier.com/locate/ejcb

Research paper

Tetramethylpyrazine induces SH-SY5Y cell differentiation toward the neuronal phenotype through activation of the PI3K/Akt/Sp1/TopoIIβ pathway

Yong-xin Yan[a], Jun-xia Zhao[a], Shuo Han[b], Na-jing Zhou[a], Zhi-qiang Jia[a], Sheng-jie Yao[a], Cui-li Cao[b], Yan-ling Wang[a], Yan-nan Xu[a], Juan Zhao[a], Yun-li Yan[a,*], Hui-xian Cui[b,c]

[a] Department of Cell Biology, Hebei Medical University, Hebei, PR China
[b] Department of Human Anatomy, Hebei Medical University, Hebei, PR China
[c] Hebei Key Laboratory for Brain Aging and Cognitive Neuroscience, Hebei, PR China

ARTICLE INFO

Article history:
Received 6 April 2015
Received in revised form 9 September 2015
Accepted 30 September 2015

Keywords:
Tetramethylpyrazine
Neuronal differentiation
TopoisomeraseIIβ
PI3K/Akt
Specificity protein 1
SH-SY5Y cell

ABSTRACT

Tetramethylpyrazine (TMP) is an active compound extracted from the traditional Chinese medicinal herb Chuanxiong. Previously, we have shown that TMP induces human SH-SY5Y neuroblastoma cell differentiation toward the neuronal phenotype by targeting topoisomeraseIIβ (TopoIIβ), a protein implicated in neural development. In the present study, we aimed to elucidate whether the transcriptional factors specificity protein 1 (Sp1) and nuclear factor Y (NF-Y), in addition to the upstream signaling pathways ERK1/2 and PI3K/Akt, are involved in modulating TopoIIβ expression in the neuronal differentiation process. We demonstrated that SH-SY5Y cells treated with TMP (80 μM) terminally differentiated into neurons, characterized by increased neuronal markers, tubulin βIII and microtubule associated protein 2 (MAP2), and increased neurite outgrowth, with no negative effect on cell survival. TMP also increased the expression of TopoIIβ, which was accompanied by increased expression of Sp1 in the differentiated neuron-like cells, whereas NF-Y protein levels remained unchanged following the differentiation progression. We also found that the phosphorylation level of Akt, but not ERK1/2, was significantly increased as a result of TMP stimulation. Furthermore, as established by chromatin immunoprecipitation (ChIP) assay, activation of the PI3K/Akt pathway increased Sp1 binding to the promoter of the TopoIIβ gene. Blockage of PI3K/Akt was shown to lead to subsequent inhibition of TopoIIβ expression and neuronal differentiation. Collectively, the results indicate that the PI3K/Akt/Sp1/TopoIIβ signaling pathway is necessary for TMP-induced neuronal differentiation. Our findings offer mechanistic insights into understanding the upstream regulation of TopoIIβ in neuronal differentiation, and suggest potential applications of TMP both in neuroscience research and clinical practice to treat relevant diseases of the nervous system.

1. Introduction

Tetramethylpyrazine (TMP), also called *ligustrazine*, is a biologically active alkaloid isolated from the traditional herbal medicine *Ligusticum wallichii Franch*. It has long been used in clinical practice to improve circulation and prevent clot formation (Xu et al., 2003). It is well known that TMP acts as a calcium channel antagonist (Pang et al., 1996) or as an antioxidant (Yang et al., 2008). Recently, TMP has received attention for its distinctive roles in stimulating neurogenesis after focal ischemia in the rat brain (Xiao et al., 2010), inducing neuronal differentiation of rat neural stem cells (Tian et al., 2010) and displaying neuro-protective roles in traumatic spinal cord injury (Hu et al., 2013) and chronic hypoxia of the medulla oblongata in a rat model (Ding et al., 2013), in addition to improving scopolamine-induced memory impairment (Wu et al., 2013). These results suggest TMP as a promising candidate for therapy in relevant neurologic disorders. However, the molecular mechanism underlying TMP's functional roles in the human nervous system, especially TMP's stimulus of neurogenesis or neuronal differentiation, needs to be further investigated.

Abbreviations: ChIP, chromatin immunoprecipitation; DMEM, Dulbecco's modified Eagle's medium; DMSO, dimethyl sulfoxide; ERK1/2, extracellular signal-regulated kinase 1/2; LDH, lactate dehydrogenase; MAP2, microtubule associated protein 2; MTT, 3-(4,5-dimethylthiazol-2-yl)-2,5-dipheny tetrazolium bromide; NF-Y, nuclear factor Y; PBS, phosphate-buffered saline; PCR, polymerase chain reaction; PI3K, phosphatidylinositol 3-kinase; Sp1, specificity protein 1; TBS, Tris-buffered saline; TMP, tetramethylpyrazine; TopoII, topoisomeraseII.

* Corresponding author at: Department of Cell Biology, Institute of Basic Medicine, Hebei Medical University, 361 Zhongshan East Road, Shijiazhuang 050017, China.
E-mail address: yanyunli2015@163.com (Y.-l. Yan).

http://dx.doi.org/10.1016/j.ejcb.2015.09.001
0171-9335/

DNA topoisomerasesII (TopoII) are ATP-dependent enzymes that alter DNA topology by cleavage and re-ligation of the DNA. Eukaryotic TopoII exists as two isoforms named TopoIIα and TopoIIβ (Austin and Marsh, 1998). They are encoded by the TOP2A and TOP2B genes located on chromosomes 17q21 ± 22 and 3p24, respectively (Forterre et al., 2007; Tan et al., 1992). Although both enzymes are highly homologous, they are genetically distinct and exhibit different patterns of expression and cellular function. Expression of TopoIIα is cell cycle-dependent, and essential for DNA replication and chromosome segregation in mitotic cells (Turley et al., 1997; Wang, 2002), whereas TopoIIβ levels remain unchanged during cell cycle progression, and are maximal in terminally differentiated tissues (Turley et al., 1997; Vávrová and Šimůnek, 2012). Recent studies have determined that TopoIIβ is a critical molecule in neuronal differentiation (Isik et al., 2015; Tsutsui et al., 2001). It plays a pivotal role in neural development (Yang et al., 2000) and axon guidance (Nur-E-Kamal et al., 2007). The transcriptional induction that is dependent on TopoIIβ may be specific to neuronal genes (Heng and Le, 2010; Lyu et al., 2006). Moreover, it has been shown that TopoIIβ regulates transcription of neuronal genes by directly binding to their regulatory regions, and emerged as an epigenetic regulator of transcription in later-stage neural development (Lyu et al., 2006; Tiwari et al., 2012).

The transcription of the TopoIIβ gene is regulated mainly by a region between −553 and −481 relative to the transcription start site, with binding sites for specificity protein 1 (Sp1) and nuclear factor Y (NF-Y) on the gene promoter (Lok et al., 2002). In previous studies, we have reported that Sp1 regulates TopoIIβ expression in SH-SY5Y cells during retinoic acid-induced neuronal differentiation (Guo et al., 2014). We also demonstrated that TMP promotes SH-SY5Y cell differentiation via enhanced TopoIIβ expression, which is mediated by transcriptional activation of TopoIIβ through increased association of acetylated histones H3 and H4 with the TopoIIβ gene promoter. These epigenetic alterations on the TopoIIβ gene structure may lead to an open chromatin state for transcription factor access (Yan et al., 2014). However, whether TMP induces neuronal differentiation of SH-SY5Y cells via Sp1 or NF-Y to regulate TopoIIβ gene expression, as well as related upstream signaling molecules, need to be clearly determined.

Currently, accumulating evidence has indicated that neuronal differentiation is regulated by several cell signaling molecules, including phosphatidylinositol 3-kinase (PI3K)/Akt (Chan et al., 2013; Lopez-Carballo et al., 2002) and the extracellular signal-regulated protein kinase 1/2 (ERK 1/2) pathways (Tian et al., 2010; Tsao et al., 2013). ERK1/2 is considered to be able to induce neurogenesis by regulating certain genes mediated by Sp1 (Dore et al., 2009), and the PI3K/Akt/Sp1 pathway is also positively correlated to cellular differentiation (Takao et al., 2012; Yin et al., 2012). Moreover, previous studies have shown that TMP impacts on different cellular functions through both the PI3K/Akt and ERK1/2 pathways (Lv et al., 2012; Tian et al., 2010; Zhang et al., 2014). Recently, direct evidence has shown that the ERK1/2 signaling pathway is involved in TMP-induced differentiation of rat neural stem cells into neurons (Tian et al., 2010).

To unravel the relationship between these signaling molecules and TopoIIβ gene expression during TMP-induced neuronal differentiation, the present study used human SH-SY5Y neuroblastoma cells as a differentiating model. Following 3–5 days' treatment with TMP (80 μM), the cells were shown to terminally differentiate into neurons through upregulation of TopoIIβ. PI3K/Akt signaling, but not ERK1/2, is required for this differentiation process. We further demonstrated a positive connection between the PI3K/Akt signal and the increased expression of TopoIIβ mediated by Sp1, suggesting that TMP induces neuronal differentiation through interactions with the PI3K/Akt/Sp1/TopoIIβ signaling pathway. In contrast to Sp1, NF-Y was found to be independent of both PI3K/Akt and ERK1/2 signals, and levels remained unchanged following the differentiation process. Unexpectedly, using chromatin immunoprecipitation (ChIP), we found increased NF-Y binding to the TopoIIβ promoter. The possible role of NF-Y in transcription of the TopoIIβ gene during TMP induction of neuronal differentiation is also discussed in this study.

2. Materials and methods

2.1. Regents and antibodies

TMP was purchased from Sigma (St. Louis, MO, USA) and was dissolved in dimethylsulfoxide (DMSO; Sinopharm Chemical Reagent Co., Ltd., Shanghai, China). The chemical structure of TMP is shown in Fig. 1A. The cell proliferation assay kit 3-(3,4-dimethylthiazol-2-yl)-2,5-diphenyltetrazolium bromide (MTT) was purchased from Roche Diagnostics (Mannheim, Germany). We purchased nuclear dye 4′,6-diamidino-2-phenylindole (DAPI) from Sigma (St. Louis, MO, USA). The fetal bovine serum (FBS), 0.25% trypsin-EDTA, and a penicillin/streptomycin mixture were obtained from Gibco-BRL (Grand Island, NY, USA). Cell cycle analysis kits were from Roche Applied Science (Indianapolis, IN, USA). We purchased rabbit anti-cleaved-caspase-3, anti-phospho-Akt (Ser473) and anti-phospho-ERK1/2 (Thr202/Tyr204) antibodies from Cell Signaling (Boston, MA, USA). We purchased rabbit anti-Akt (Ser473) antibody from Epitomics (Burlingame, CA, USA). We purchased rabbit anti-MAP2, rabbit anti-β-actin, rabbit anti-tubulin βIII, rabbit anti-TopoIIα, rabbit anti-TopoIIβ and rabbit anti-ERK 1/2 antibodies from Bioworld Technology, Inc. (Minneapolis, MN, USA). Rabbit anti-Sp1 antibody was obtained from Abcam (Cambridge, MA, USA). Rabbit anti-NF-YA antibody and all secondary antibodies against mouse and rabbit IgG were purchased from Santa Cruz Biotechnology Inc. (Santa Cruz, CA, USA). MEK inhibitor U0126 was purchased from Calbiochem (San Diego, CA, USA). PI3K inhibitor LY294002 was purchased from Calbiochem (Merck, Germany). They were all diluted in DMSO. LDH Cytotoxicity Assay Kits and ChIP assay kits were obtained from Beyotime Biotechnology Institute (Shanghai, China). The eukaryotic protein synthesis inhibitor cycloheximide (CHX) was obtained from Sigma Chemical Co. (St. Louis, MO, USA). The catalytic inhibitor of TopoIIβ ICRF-193, bis (2,6-dioxopiperazine) and the RNA polymerase II inhibitor α-amanitin were purchased from Santa Cruz Biotechnology Inc. (Santa Cruz, CA, USA).

2.2. Cell culture and differentiation induction

SH-SY5Y Cells were cultured in Dulbecco's modified Eagle's medium (DMEM), supplemented with 10% fetal bovine serum (FBS), 2 mM L-glutamine, 100 units/mL of penicillin and 100 μg/mL of streptomycin in a 37 °C humidified incubator with an atmosphere of 5% CO_2 in air. For promotion of neuronal differentiation, the cells were cultured with an inducing medium composed of 80 μM TMP in DMEM with 3% FBS as described in previous studies (Tian et al., 2010; Yan et al., 2014), and an equal volume of DMSO was added for the control cells. The control and TMP-treated cells were cultured for 5 days, changing the fresh medium every two days. Except for the TMP exposure, all control cells were handled in parallel with the test cells.

2.3. Cell viability measured by MTT assay

SH-SY5Y cells in the logarithmic growth phase were seeded in a 96-well culture plate with 1×10^4 cells/well. Twenty-four hours after plating, 0, 10, 20, 40, 80 and 120 μM TMP were used respectively to treat cells and growth was evaluated on days 0 to 5. At each time point, 20 μL MTT (5 mg/mL) was added into the 200 μL

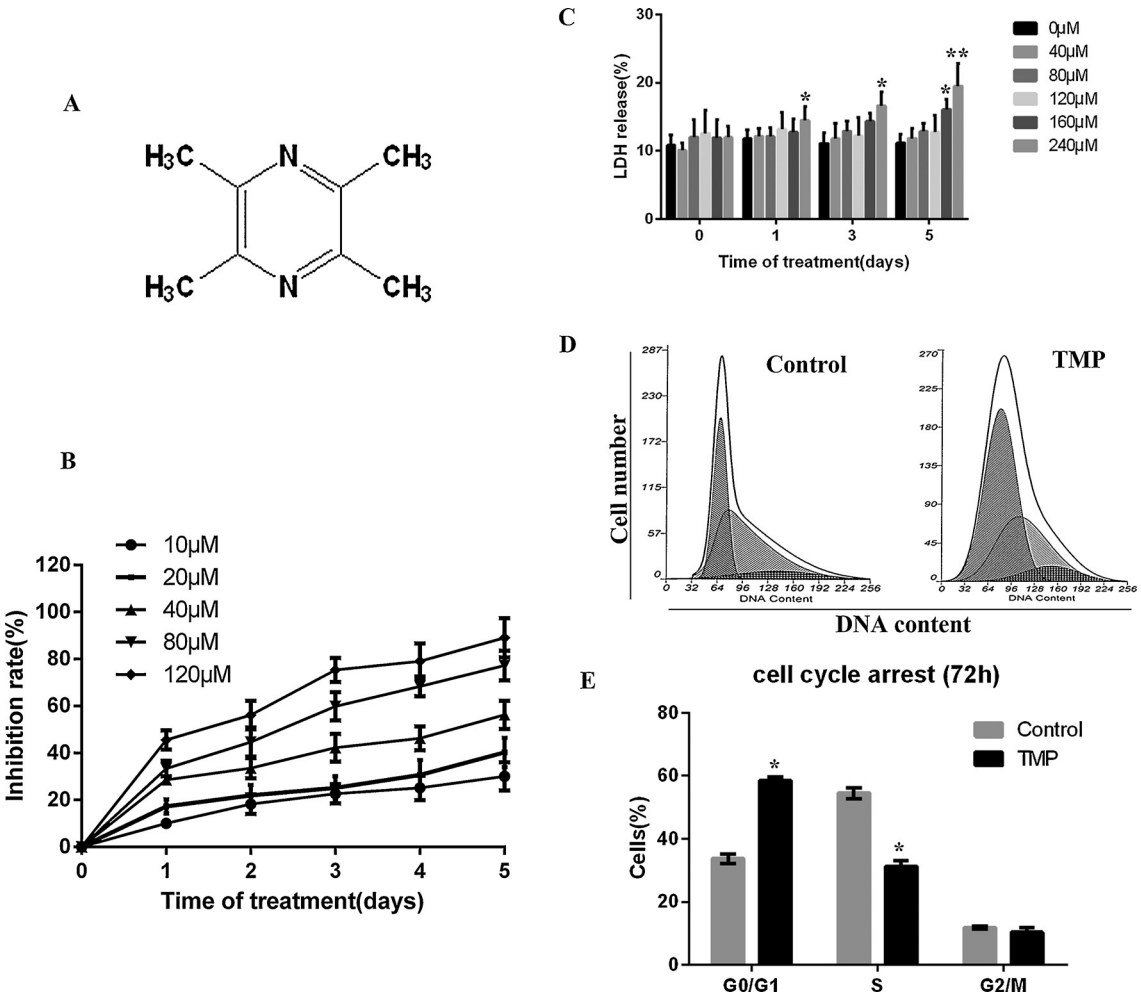

Fig. 1. TMP's effect on the growth and LDH release of SH-SY5Y cells. (A) The chemical structure of TMP. (B) Dose and time dependent inhibition of TMP on SH-SY5Y cells determined by MTT assay. Cells were seeded in 96-well plates at a density of 1×10^4 cells/well. After treatment with TMP in indicated concentrations for indicated time, the cell growth was evaluated through detecting absorbance at 490 nm. Each point was done in sextuplicate and the experiment was repeated three times. (C) LDH release assay. Cells were treated with various concentrations of TMP for 0, 1, 3 and 5 days. LDH release was determined using the LDH assays. The absorbance of all samples was measured at 490 nm with a microplate reader. LDH release was expressed as percentage of total LDH activity (LDH in the medium + LDH in the cell) according to the following equation: % LDH release = (LDH activity in the medium/total LDH activity) × 100. (D, E) The effects of TMP on cell cycle progression in SH-SY5Y cells. Cells treated with TMP were stained with propidium iodide and DNA contents of cells were measured by flow cytometry analysis. Typical cytograms are presented that represent the overlaps of the percentage of cells in each phase (G_0/G_1, S, and G_2/M). This analysis indicates that TMP treated cells were arrested at G_0/G_1 phase compared with the untreated control cells. Diagram showing an accumulation of cells at G_0/G_1 phase of the cell cycle following TMP treatment at a concentration of 80 μM on the 3rd days. Error bars indicate the standard deviation (SD) of the mean. The asterisk represents statistically different from the corresponding control values (*$P < 0.05$ vs. control, **$P < 0.01$ vs. control).

of culture medium in each well. Four hours later, the medium was removed and 150 μL DMSO was added into each well in order to dissolve the precipitate. Absorbance (A) was measured at 490 nm using an automated microplate reader (ELX800, Bio-Tek, USA). Three independent experiments were repeated in each group. Cell viability was calculated according to the following formula: inhibition rate (%) = $1 - (A_{TMP} - A_{blank})/(A_{control} - A_{blank}) \times 100\%$ (A: average absorbance under 490 nm).

2.4. Lactate dehydrogenase (LDH) release assay

We measured extracellular and intracellular LDH activity spectrophotometrically using an LDH Cytotoxicity Assay Kit (Beyotime Institute of Biotechnology, Shanghai, China) according to the manufacturer's instructions. Cells were plated in a black, clear-bottom 96-well plate and treated with TMP concentrations ranging from 0 to 240 μM. SH-SY5Y cells (1×10^4 cells/well) were incubated at 37 °C for 0, 1, 3 and 5 days with or without TMP treatment. The supernatant was aspirated and mixed with 60 μL of the reaction solution in each well and incubated for up to 30 min at room temperature with slow shaking. The absorbance of all samples was measured at 490 nm with a microplate reader (ELX800, Bio-Tek, USA). LDH release was expressed as percentage of total LDH activity (LDH in the medium + LDH in the cells) according to the following equation: % LDH release = (LDH activity in the medium/total LDH activity) × 100%.

2.5. Cell cycle analysis

We examined the effects of TMP on cell cycle distribution using flow cytometry. Cells were collected and washed twice with ice-cold phosphate-buffered saline (PBS). The cells were fixed and permeabilized with 70% ice-cold ethanol at 4 °C for 1 h. After washing once with PBS, the cells were resuspended in a staining solution containing propidium iodide (50 μL/mL) and RNase A (250 μg/mL). The cell suspensions were then incubated for 30 min at room temperature before being detected by an EPICS-XL™ flow cytometer (Beckman Coulter, Brea, CA, USA), using at least 10,000 cells for each group. Data were analyzed using MultiCycle AV software (Phoenix

Flow Systems, San Diego, CA, USA). Experiments were repeated at least three times.

2.6. DAPI staining assay and caspase-3 activity assay

DAPI fluorescent dye was used to detect DNA condensation and nuclear fragmentation, which are characteristic of apoptotic cells. We seeded 1×10^5 cells/well in 6-well plates on coverslips for 24 h. Cells were incubated with/without 80 μM TMP treatment for 0, 1, 3 and 5 days, washed with PBS, and fixed with 4% paraformaldehyde for 15 min. After staining with DAPI (5 μg/mL) for 15 min, the cells were observed under a fluorescence microscope (IX71, Olympus Optical Co., Ltd., Tokyo, Japan).

Activity of caspase-3 was measured using a caspase-3 activity detection kit according to the manufacturer's instructions (Millipore, Billerica, MA, USA). In brief, SH-SY5Y cells (1×10^5 cells/well) were treated with 80 μM TMP for 0, 1, 3 and 5 days. The cells were lysed in the supplied lysis buffer and incubated for 10 min on ice, and then centrifuged at 10,000 × *g* for 5 min. The supernatant was collected and incubated with assay buffer and caspase-3 substrate (Ac-DEVD-pNA) for 1.5 h at 37 °C. The optical density of the reaction mixture was quantified using an automated microplate reader (ELX800, Bio-Tek, USA) at 405 nm.

2.7. Measurement of neurite outgrowth and evaluation of neurite-bearing cells

Cells were cultured in poly-L-lysine (PLL)-coated 6-well plates and induced to differentiate for up to 5 days with 80 μM TMP. Neurite outgrowth was observed under phase contrast microscopy image acquisition (Olympus IX71 equipped with a DP73 CCD digital camera, Japan). Neurite length measurements were made on the time-lapse sequences obtained, using the NeuronJ plugin (Wayne Rasband, National Institute of Mental Health, Bethesda, MD, USA) from ImageJ software (National Institutes of Health, Bethesda, MD, USA) on 100 cells in each experiment. Cells were considered to be differentiated when the total neurite length was longer than 100 μm for each cell (Yan et al., 2014) (Oe et al., 2005). The average total neurite length for each experimental condition was determined from at least 100 ($n = 100$) randomly selected cells in each group. The percentage of differentiated cells per culture condition was also calculated.

2.8. ERK1/2 and PI3K/Akt inhibitor treatments

A 10 mM stock solution each of LY294002 (a specific PI3K inhibitor) and U0126 (a specific MEK1/2 inhibitor) were prepared in DMSO, stored at −20 °C in the dark, and diluted with medium just before use. Cells were seeded in 6-well plate in a relatively low density (10,000 cells/well) in triplicate and grown in DMEM medium containing 10% FBS. One day following the plating, the cells were pre-incubated for 60 min with either 10 μM LY294002 or 10 μM U0126 before the addition of culture medium containing 80 μM TMP. The cells were then cultured continuously for 5 days. Fresh inducing medium was provided every 2 days.

2.9. Western blot analysis

Cells were grown in 60 mm polystyrene dishes at an initial seeding density of 1.5×10^5 cells per dish. After TMP treatment, cells were collected and rinsed with ice-cold PBS. Proteins were extracted using Pierce Nuclear and Cytoplasmic Extraction Reagents (Pierce Biotechnology, Inc., Rockford, USA) and analyses were performed according to the standard procedure supplied in the manufacturer's instructions. Cell lysates were heated at 100 °C for 8 min and separated by electrophoresis through 6–15% SDS-polyacrylamide gels. Following electrophoretic transfer of proteins to PVDF membranes using a wet transfer apparatus (Bio-Rad, Hercules, CA), membranes were blocked in 5% (wt/vol) nonfat dry milk in TBS (Tris-buffered saline) containing 0.1% (v/v) Tween-20 for 30 min at room temperature. The membranes were incubated with specific primary antibodies at 4 °C overnight. After washing with TBS three times (10 min each time), membranes were incubated for 1 h with appropriate horseradish peroxidase-conjugated secondary antibodies at 37 °C. Protein bands were visualized using an enhanced chemiluminescence Western blotting kit (ECL; Amersham, Inc, United Kingdom) and captured using ChemiScope3600 Mini chemiluminescence imaging systems (Clinx Science Instruments Co., Ltd., Shanghai, China). Analyses of band densities were performed using version 1.48 of ImageJ software (National Institutes of Health, Bethesda, MD, USA). All fold changes in band densities were determined relative to β-actin, which was used as a loading control.

2.10. RNA extraction and reverse transcription polymerase chain reaction (RT-PCR)

Total RNA was extracted from SH-SY5Y cells using Trizol reagent (Sigma, St. Louis, MO, USA) according to the manufacturer's instructions. First strand cDNA was synthesized from 1 μg RNA, using a cDNA reverse transcription kit (GeneCopoeia Inc., MD, USA) following manufacturer's instructions, and the synthesized cDNA was stored at −20 °C until use. PCR was performed using the Golden Easy PCR System (KT221; Tiangen, Beijing, China). The PCR primers for TopoIIα were 5′-GATAGGAGCAGTGACGA-3′ (forward) and 5′-GCGGCGATTCTTG-3′ (reverse). The PCR primers for TopoIIβ were: 5′-AGCCGAAAGACCTAAA-3′ (forward) and 5′-TGAATCCGAGTCAGAGTT-3′ (reverse). The PCR primers for β-actin were 5′-GTGGACATCCGCAAAGAC-3′ (forward) and 5′-GAAAGGGTGTAACGCAACTA-3′ (reverse). The standard PCR amplification was carried out for 30 cycles, each cycle consisting of denaturation at 94 °C for 1 min, annealing at 55.6 °C for 1 min, and extension at 72 °C for 1.5 min. β-Actin served as an internal control. Each experiment was repeated three times independently. Amplified products were separated on 1.5% agarose gel and stained with Goldview (SBSgene, Beijing, China). The bands were photographed under a UV transilluminator (G-BOX; Syngene, Cambridge, United Kingdom) and the relative mRNA expression levels were quantified densitometrically using an image analysis system (G-BOX; Syngene, Cambridge, United Kingdom). Relative mRNA levels of the target genes were calculated in comparison with the reference bands of β-actin. Real-time quantitative PCR for confirmation of the TopoII cDNA is described in Section 2.12.

2.11. ChIP assay

ChIP assay was performed based on a method previously described (Yan et al., 2014), using the manufacturer's instructions for the ChIP assay kit (Beyotime Biotechnology Institute, Shanghai, China) with appropriate modifications. Cells were seeded and grown in 6-well plates with 10 mL of culture medium for 0, 1, 3 and 5 days. Protein-DNA cross-linking was obtained by adding formaldehyde at a final concentration of 1% for 20 min. Thereafter, cells were washed twice with cold PBS. Cross-linking was stopped by the addition of 1.1 mL glycine solution (10×), and cells were harvested and resuspended in 200 μL (per 10^7 cells) of SDS lysis buffer following 10 min incubation on ice. Lysis of the cells was performed by grinding with acid-washed glass beads. Fixed chromatin was sonicated using a Scientz98-III non-contact type ultrasonic cell crusher (Scientz, Shanghai, China) on ice for 30 min to a fragment size of 300–1000 bp. After centrifugation,

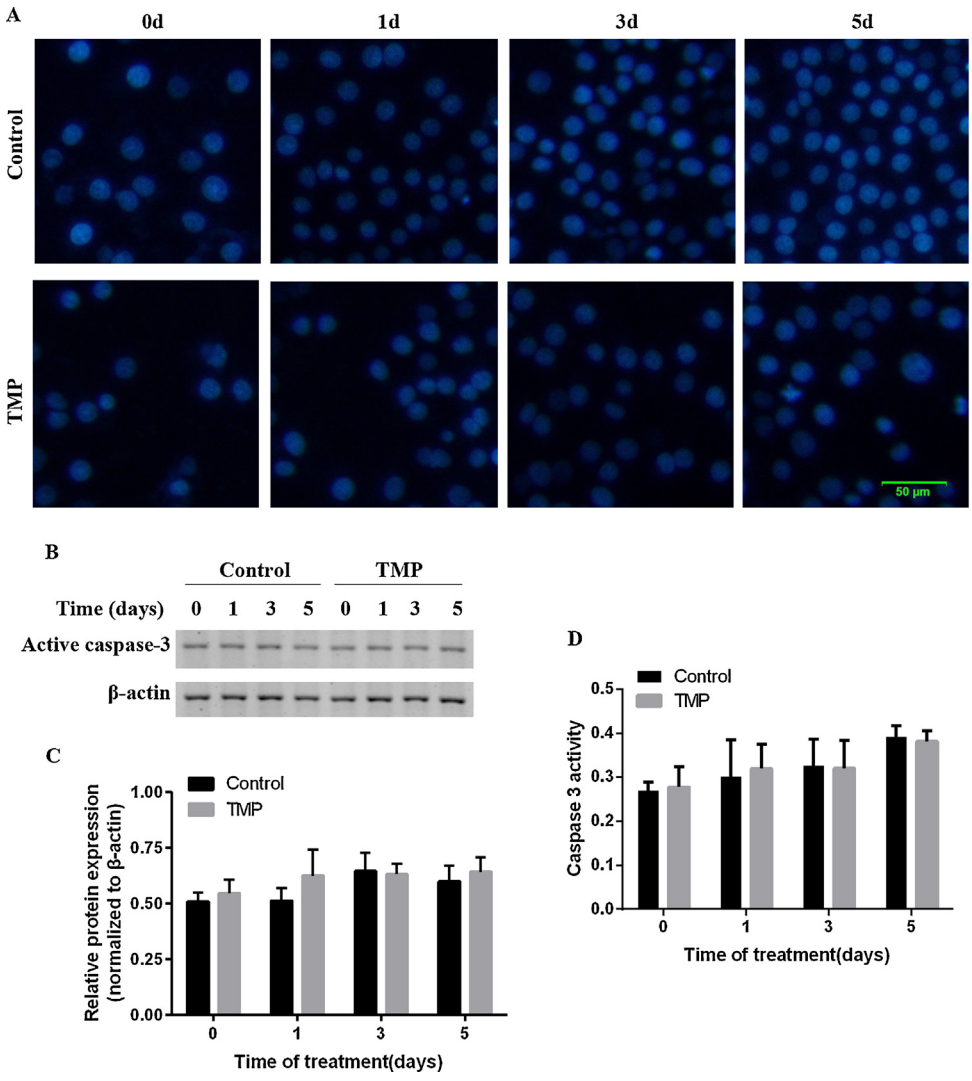

Fig. 2. Detection of DNA condensation and apoptosis in SH-SY5Y cells. (A) The nuclear morphologies of cells treated with TMP. Cells were treated with 80 μM TMP for 0, 1, 3 and 5 days, followed by nuclear staining with DAPI and then cells were examined using fluorescence microscopy. The images shown are representative of three experiments. Scale bar represents 50 μm. (B) Active caspase-3 protein expression following treatment with 80 μM TMP. Cells were harvested on indicated days. Cellular extracts were subjected to Western blot with antibodies specific for active caspase-3. The results shown are representative Western blots of at least three independent experiments. (C) Densitometric analysis of bands representing means ± SD of three independent experiments. β-Actin was used as loading control. (D) Caspase-3 activity evaluation. Activity of caspase-3 was measured using a caspase-3 activity detection kit according to the manufacturer's instructions. SH-SY5Y cells (1×10^5 cells/well) were treated with 80 μM TMP for 0, 1, 3 and 5 days and whole cells were lysed in the supplied lysis buffer and incubated for 10 min on ice. The supernatant were collected and incubated with assay buffer and caspase-3 substrate (Ac-DEVD-pNA) for 1.5 h at 37 °C. The optical density of the reaction mixture was quantified using an automated microplate reader at 405 nm. Error bars indicate the standard deviation (SD) of the mean.

immunoprecipitation was performed using 200 μL of the sonicated chromatin solution and either 1 μL rabbit anti-Sp1 or NF-YA antibodies, or no antibody as a negative control, incubated overnight at 4 °C with rotation. Purification of the immunoprecipitated protein/DNA complexes was achieved by adding 60 μL of slurry protein *A*+*G* Agarose/Salmon Sperm DNA for a minimum of 60 min. Following binding, precipitates were washed with low salt, high salt, LiCl Immune Complex wash buffer and finally TE buffer. Elution of bound protein/DNA was achieved by 30-min incubation with 250 μL of elution buffer (1% SDS, 0.1 M $NaHCO_3$) prewarmed to 65 °C. DNA was uncrosslinked for a minimum of 6 h by incubation in 5 M NaCl at 65 °C followed by purification and ethanol precipitation. All samples were treated with RNase A and proteinase K (Roche Diagnostics, Mannheim, Germany). DNA was recovered by extraction in phenol/chloroform/isoamyl alcohol followed by ethanol precipitation. Immunoprecipitated DNA samples were resuspended in H_2O and fractions used for semi-quantitative PCR or real-time PCR. DNA was quantified by semi-quantitative PCR which was performed using the Golden Easy PCR System (KT221; Tiangen, Beijing, China). The following primers were used: 5′-AACTGTGTTCTCTGTC-3′ (forward), 5′-CTCCTGGCAAAGAATA-3′ (reverse) and 5′-CTGTGTTCTCTGTCTC-3′ (forward), 5′-CTCCTGGCAAAGAATA-3′ (reverse) for the TopoIIβ promoter flanking the Sp1 and NF-Y binding sites, respectively. Amplified products were separated on a 1.5% agarose gel and stained with Goldview (SBSgene, Beijing, China). The bands were photographed under a UV transilluminator (G-BOX; Syngene, Cambridge, United Kingdom) and the relative DNA levels were quantified densitometrically using an image analysis system (G-BOX; Syngene, Cambridge, United Kingdom). Quantitation of the DNA was calculated on the basis of normalizing against serially diluted sonicated genomic input DNA obtained in aliquots from the same chromatin preparation. Real-time PCR for confirmation of the immunoprecipitated DNA was performed as below.

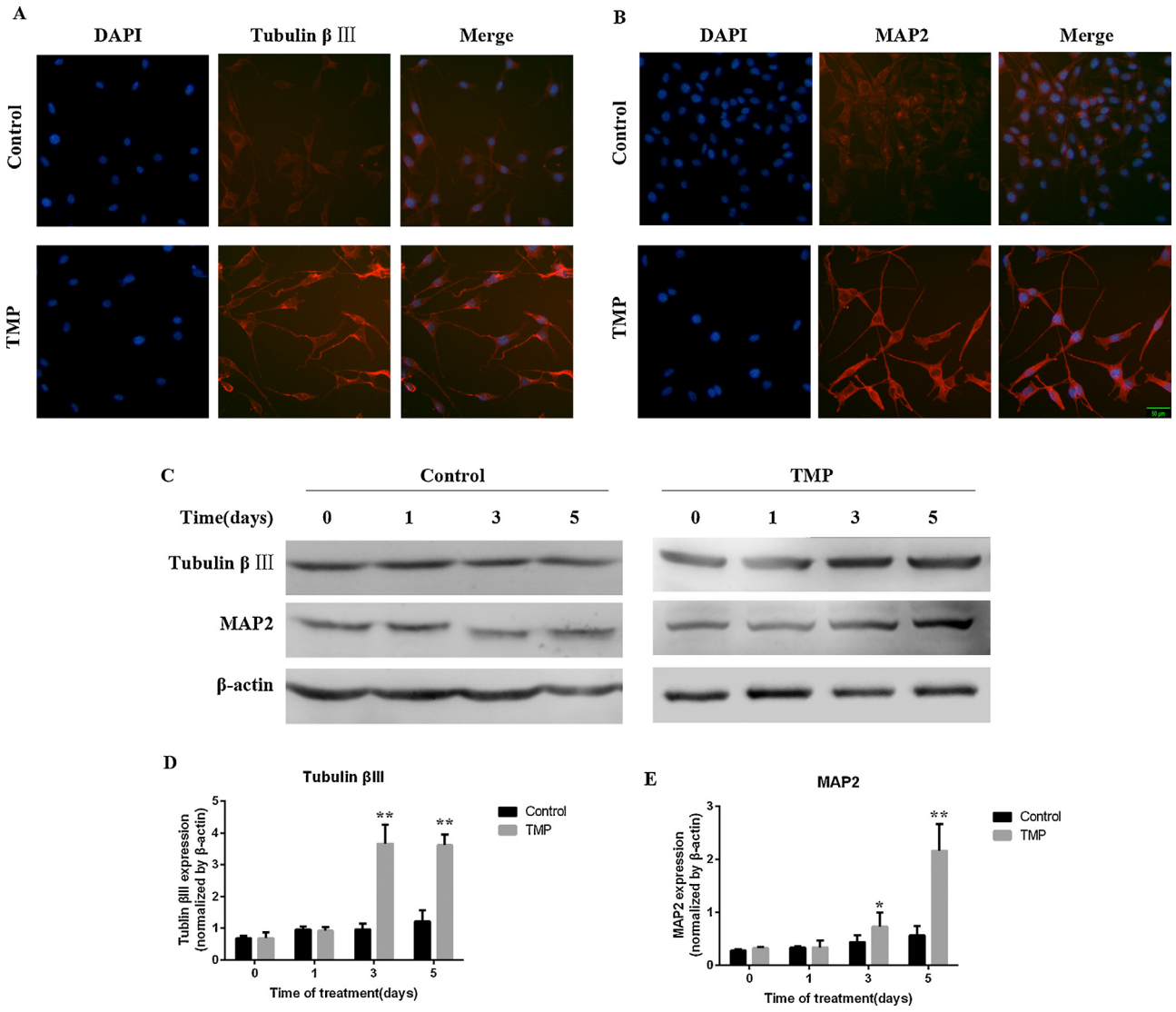

Fig. 3. TMP increased the expression of neuronal markers tubulin βIII and MAP2. (A, B) Immunofluorescent staining for neuronal markers MAP2 and tubulin βIII expression after 5 days of differentiation induced by TMP. Scale bar = 50 μm. (C–E) Tubulin βIII and MAP2 expressions during 0, 1, 3 and 5 days of differentiation induced by 80 μM TMP in SH-SY5Y cells are shown by densitometric analyses. Lyses of control cells and TMP-treated cells were subjected to Western blot analysis. The neuronal marker proteins tubulin βIII and MAP2 increased after TMP treatment. (C) Representative immunoblots of the neuronal markers tubulin βIII and MAP2. (D, E) Densitometric analysis of bands representing means ± SD of three independent experiments. β-Actin was used as loading control. Error bars indicate the standard deviation of the mean. The asterisk represents statistically different from the corresponding control values (*$P < 0.05$ vs. control, **$P < 0.01$ vs. control). (For interpretation of the references to color in this figure legend, the reader is referred to the web version of this article.)

2.12. Real-time quantitative PCR (RT-qPCR) for immunoprecipitated DNA or TopoII cDNA

For RT-qPCR, 25 μL of reaction mixture containing 1 μL of template DNA, 12.5 μL of SYBR Green, 1 μL each of the forward and reverse primers and 9.5 μL RNase-free water was added to each sample. Thirty-five amplification cycles were performed according to the program used in RT-qPCR assay. For each sample, analysis was carried out in triplicate. Real time quantitative RT-PCR with UltraSYBR Mixture (CW Biotech, Beijing, China) was performed using the Eco^{TM} quantitative PCR system (Illumina, CA, USA). The following primers were used in real-time PCR analyses for mRNA expression: TopoIIα: 5′-CCTTCTATGGTGGATGGT-3′ (forward), 5′-TTACTTCTCGCTTGTCATTC-3′ (reverse); TopoIIβ: 5′-TGGTCGTAATGGTTATGGT-3′ (forward) and 5′-ATCTGGTTGGAATGTTATGC-3′ (reverse); GAPDH: 5′-GAAGGTCGGAGTCAACGG-3′ (forward) and 5′-TGGAAGATGGTGATGGGAT-3′ (reverse). The fluorescent signals were collected during the extension phase, Ct values of the samples were calculated, and the transcription levels of TopoIIα and TopoIIβ were normalized to those of GAPDH by the $2^{-\Delta\Delta Ct}$ method.

Immunoprecipitated DNA and input DNA were analyzed by RT-qPCR using the same protocol as that used for gene expression analysis. Specific primers were designed to amplify proximal promoter regions. For Sp1, the primers to amplify the TopoIIβ promoter region were 5′-GAGAAGGTCTGAGATGAT-3′(forward) and 5′-CTCTAAGGATGAGGATGG-3′ (reverse). For NF-YA, the primers were 5′-AAGAAGGAGATGGAGAAG-3′ (forward) and 5′-TTACTCTGAGACCTAACC-3′ (reverse). The amounts of immunoprecipitated DNA were normalized against the corresponding input DNA. The results are presented as fold increases calculated by dividing the average value of the immunoprecipitated DNA by the average value of the corresponding input DNA. Each experiment was performed three times with independent chromatin extracts.

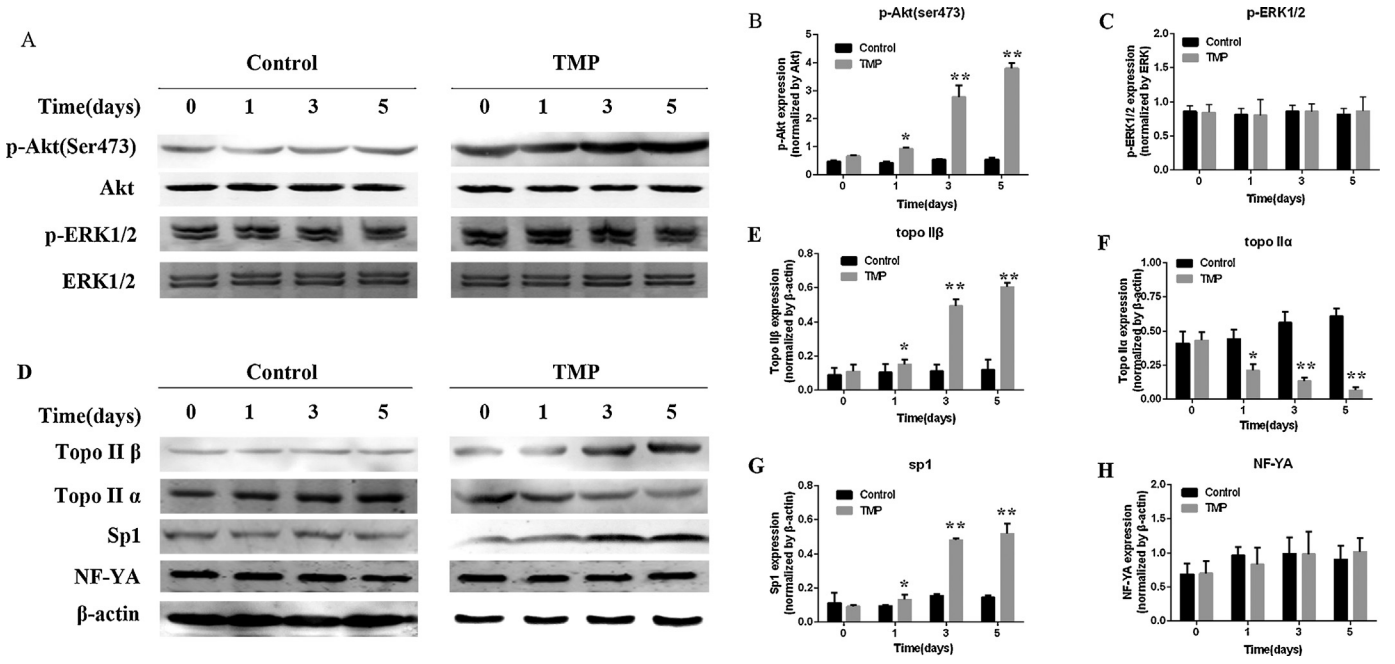

Fig. 4. TMP induced phosphorylation of PI3K/Akt was positively correlated with the expression of TopoIIβ and Sp1 in SH-SY5Y cells. SH-SY5Y cells were cultured in the presence or absence of 80 μM TMP for 0, 1, 3 and 5 days, the cells were lysed, and analyzed by immunoblot. (A) The expression of p-Akt and p-ERK1/2 after TMP treatment. The blot is representative of at least three experiments. (B, C) Densitometric analysis of bands representing means ± SD of three independent experiments. Densitometry indicated increase in p-Akt and unchanged p-ERK1/2 expression in cells cultured in the presence of TMP. β-Actin was used as loading control. Error bars indicate the standard deviation of the mean. The asterisk represents statistically different from the corresponding control values (*$P < 0.05$ vs. control, **$P < 0.01$ vs. control). (D) The expression of TopoIIα, TopoIIβ, Sp1 and NF-YA after TMP treatment. The blot is representative of at least three experiments. (E–H) Densitometric analysis of bands representing means ± SD of three independent experiments. Densitometry indicated increase in TopoIIβ and Sp1, decrease in TopoIIα and unchanged NF-YA expression in cells cultured in the presence of TMP. β-Actin was used as loading control. Error bars indicate the standard deviation of the mean. The asterisk represents statistically different from the corresponding control values (*$P < 0.05$ vs. control, **$P < 0.01$ vs. control).

2.13. Immunofluorescent staining

Cells cultured on glass coverslips were fixed in 4% PFA solution for 20 min, and then incubated in blocking buffer (10% goat serum in PBS) with 1% Triton X-100 for 30 min at room temperature (RT). Afterwards, samples were incubated with primary antibodies at 4 °C overnight and then with appropriate fluorescent probe-conjugated secondary antibodies for 1 h at RT. Nuclei were counterstained with DAPI. Images were taken by fluorescence microscope (Olympus IX71, Japan). Specific primary antibodies used include MAP2 (1:200, Abcam, ab32454) and tubulin β III (1:100, Santa Cruz, sc-51670), which was followed by incubation with appropriate secondary antibodies that were conjugated with DyLight 594 (Abbkine, Redland, CA, USA).

2.14. Statistical analysis

Statistical analysis was performed using SPSS 13.0 software. Data are presented as mean ± SD. Statistical analysis for independent samples was performed using one-way ANOVA with a post hoc Dunnett's test. P value <0.05 was considered as statistically significant.

3. Results

3.1. TMP's effects on the growth and cytotoxicity of SH-SY5Y cells

Previous studies have demonstrated that TMP concentrations lower than 200 μM show protective effects on neuronal cells in vitro without cell damage (Fu et al., 2008). Use of 50 μM TMP significantly preserved neuronal morphology and survival in retinal cell cultures following in vitro cultivation with lethal exposure to hydrogen peroxide (Yang et al., 2008). A recent study showed that 100 μM TMP can effectively promote neuron survival when treating primary cultured cerebral neurocytes (Chen et al., 2013). In addition, 80 μM TMP has been used for neuronal differentiation (Tian et al., 2010).

As an in vitro model for neuroscience research, SH-SY5Y cells can be differentiated into cells with the morphological and biochemical characteristics of mature neurons and are widely used for neurobiological studies (Agholme et al., 2010; Oe et al., 2005). Until now, TMP's effects on this cell model have not been clearly defined.

We assessed the effects of TMP on the proliferation of SH-SY5Y cells using MTT assays. Exponentially growing SH-SY5Y cells were exposed to various concentrations of TMP for 0, 1, 2, 3, 4 and 5 days. Cell growth was detected using an automated microplate reader and inhibition rates were calculated. It was demonstrated that TMP at concentrations ranging from 40 to 120 μM inhibited SH-SY5Y cell growth in a dose- and time-dependent manner (Fig. 1B).

To determine the cytotoxicity of TMP on SH-SY5Y cells, we measured extracellular and intracellular LDH activity spectrophotometrically using an LDH cytotoxicity assay. It was found that in cells incubated with 160 μM TMP for 5 days and 240 μM TMP for 1 day, LDH release was significantly increased compared to control cells. However, for cells treated with TMP at concentrations of 40 μM, 80 μM and 120 μM for up to 5 days, LDH release showed no difference compared with control cells (Fig. 1C). According to these results and those of other studies (Chen et al., 2013; Fu et al., 2008; Tian et al., 2010), 80 μM TMP was selected to induce SH-Y5Y cell differentiation in this study.

For examining the effect of TMP on cell death, DAPI staining was applied to show nuclear chromatin changes. No nuclear DNA condensation or nuclear fragmentation were detected after treatment with 80 μM TMP at indicated time points, which suggested that cells treated with this concentration of TMP did not exhibit apoptotic features (Fig. 2A). We also tested for proteolysis of cleaved

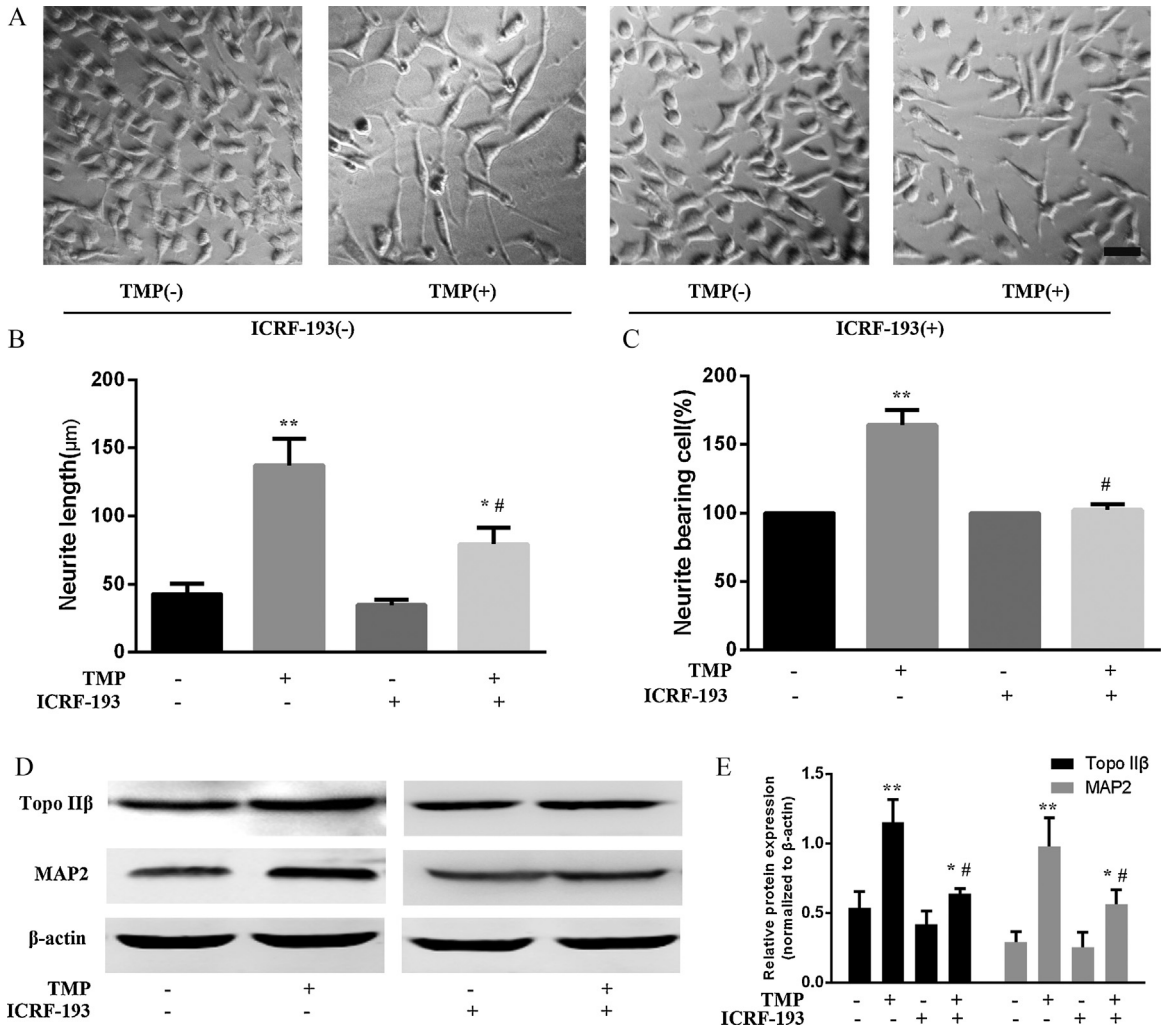

Fig. 5. ICRF-193 inhibited neurite outgrowth and neuronal marker expression in SH-SY5Y cells. (A–C) ICRF-193 inhibited TMP-induced neurite outgrowth in SH-SY5Y cells. Cells were treated with ICRF-193 at a final concentration of 40 μM and induced to differentiate with 80 μM TMP. After 5 days, neurite lengths of 100 neurons ($n = 100$) were measured as described in materials and methods. Shown are representative images of untreated, differentiated and ICRF-193 treated cells captured after 5 days of TMP treatment. Scale bar represents 50 μm. Quantification of neurite length was done in comparisons with untreated control cells. Neurite length measured by the tracing method using NeuronJ, an ImageJ add-on software. Average neurite length of at least 100 cells per condition is shown. Neurite bearing cell was quantified by counting the number of cells exhibiting neurites which were longer than 100 μm in total length. The ratio of neurite bearing cells to total cell number in TMP-untreated control cells was taken as 100%. The ratio of neurite bearing cells to total cell number in TMP-treated cells was also calculated and normalized to the corresponding control. Approximately 100 cells were counted in each medium condition. The data are expressed as the mean ± SD of three independent experiments. The asterisk represents statistically different from the corresponding control values ($^{*}P < 0.05$ vs. control, $^{**}P < 0.01$ vs. control, $^{\#}P < 0.05$ vs. TMP treated cell without ICRF-193). (D, E) ICRF-193 induced down-regulation of TopoIIβ and MAP2 in SH-SY5Y cells. Cells were seeded at a density of 1×10^5/well in a six-well culture plate and incubated for 24 h. ICRF-193 was then added to a final concentration of 40 μM respectively, and incubated for 2 h. Cells were then treated with 80 μM TMP to induce differentiation. Cells were collected 5 days after TMP treatment and lysed in for Western blot analysis. (D) Shown are representative immunoblots of TopoIIβ and MAP2 protein down-regulated by ICRF-193 in a dose dependent manner. (E) Densitometric analysis of bands representing means ± SD of three independent experiments. β-Actin was used as loading control. Error bars indicate the standard deviation of the mean. The asterisk represents statistically different from the corresponding control values ($^{*}P < 0.05$ vs. control, $^{**}P < 0.01$ vs. control, $^{\#}P < 0.05$ vs. TMP treated cell without ICRF-193).

caspase-3, one of the indicators of apoptosis (Anderton et al., 2011), using Western blot analysis and caspase-3 activity assay. Results revealed that 80 μM TMP had no effects on caspase-3 expression and caspase-3 activity in SH-SY5Y cells compared to control cells (Fig. 2B–D). The data indicate that 80 μM of TMP is a safe concentration for induction of SH-SY5Y cell differentiation.

3.2. TMP induced cellular differentiation by G_0/G_1 cell cycle arrest

It is reported that cell cycle exit at the G_1 phase is important in understanding the process of neuronal cell development (Tsuda and Lim, 2014). In this study, using flow cytometry, we analyzed the cell cycle distribution on the third day after 80 μM TMP treatment. Results showed that untreated cells displayed the typical profile of an asynchronously growing population, with 54.5% of the cells traversing S-phase. After 3 days of TMP treatment, there was a significant depletion of cells in the S and G_2/M phases (54.5% to 31.2% and 11.8% to 10.4%, respectively) and an increase in the G_0/G_1 phase (33.7% to 58.4%) of the cell cycle (Fig. 1D and E). Thus, TMP treatment induced cell cycle arrest at the G_0/G_1 phase. This agreed with the results of our previous study (Yan et al., 2014), and suggested a transition state of the cells from proliferation to differentiation.

3.3. Neuronal differentiation identified by neurite outgrowth and neuronal markers accompanied by increased TopoIIβ and decreased TopoIIα

Neurite extension is a reliable feature of neuronal differentiation (Kurauchi et al., 2011; Nur-E-Kamal et al., 2007). To define the differentiation of SH-SY5Y cells into neurons, neurite extension

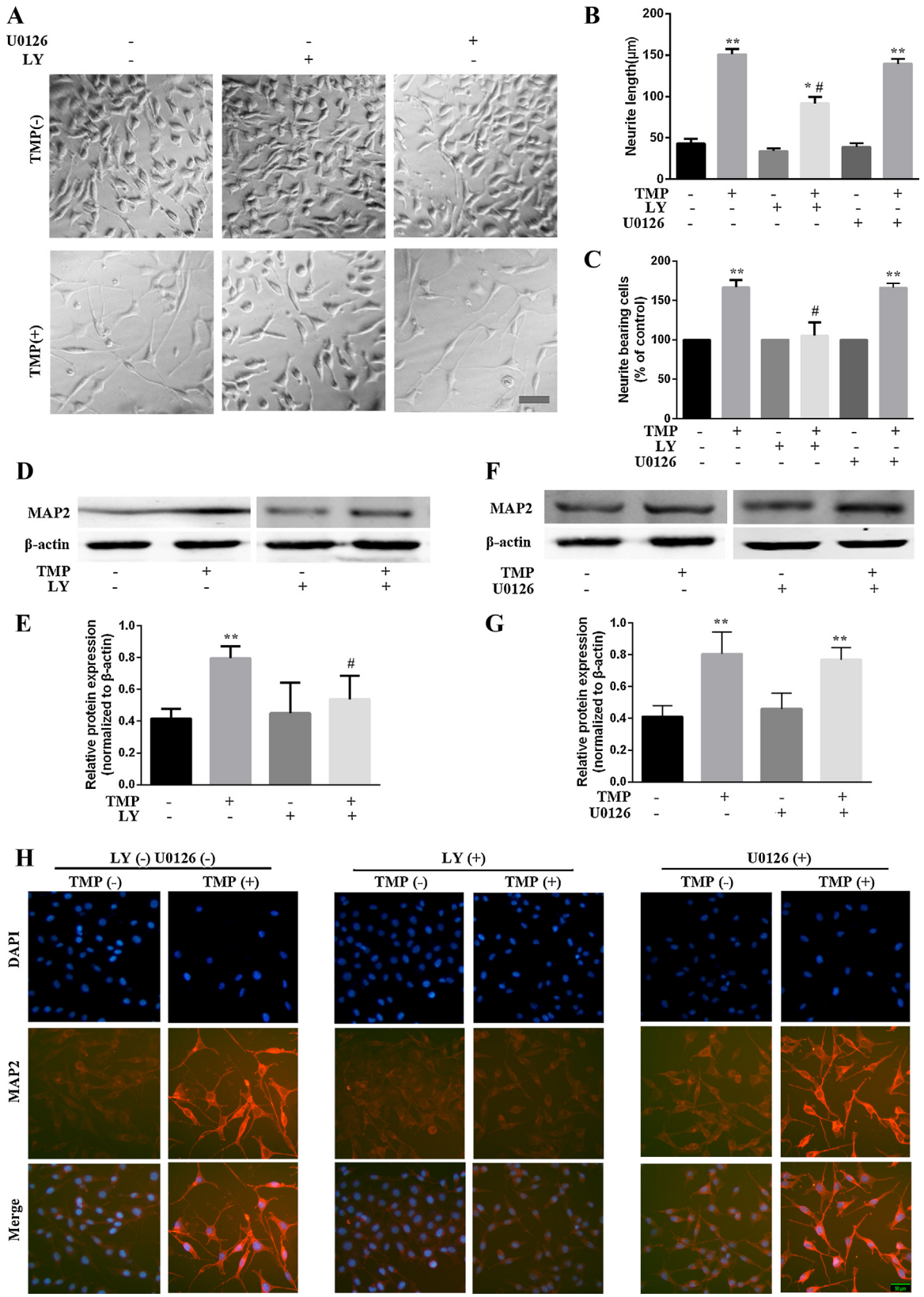

Fig. 6. LY294002 inhibited TMP-induced neurite outgrowth and neuronal markers of SH-SY5Y cells. (A–C) LY294002 (LY) inhibited TMP-induced neurite outgrowth in SH-SY5Y cells. TMP induced longer neurites relative to control cells. Neurite outgrowth in SH-SY5Y cells was harmed by PI3K/Akt chemical inhibitor LY294002. The chemical inhibitor of MEK1/2 U0126 had no effects on the neurite outgrowth. (A) Representative images of proliferative, differentiated and LY294002 treated SH-SY5Y cells on the 5th days are shown. Note the stellate morphology and the abundance of longer neurites in differentiated cells. Scale bar represents 50 μm. (B, C) Quantification of neurite length and neurite bearing cells in varies treated cells. Cells were treated with TMP with or without the inhibitors for up to 5 days. Neurite length measured by the tracing method using NeuronJ, an ImageJ add-on software. Average neurite length of at least 100 cells per condition is shown. Neurite bearing cell was quantified by counting the number of cells exhibiting neurites which were longer than 100 μm in total length. The ratio of neurite bearing cells to total cell number in TMP-untreated control cells was taken as 100%. The ratio of neurite bearing cells to total cell number in TMP-treated cells was also calculated and normalized to the corresponding control. Approximately

was measured in this study using a neurite outgrowth assay. After treatment with 80 μM TMP, cells exhibited distinct morphological changes consistent with neuronal differentiation as evidenced by development of long, out-branched neurites. Both the number and length of neurites increased during the period of neuronal differentiation (Figs. 3A and B, 5A–C and 6A–C, H). Moreover, the differentiated cells resembled primary neurons when evaluated by neuronal markers, using anti-tubulin βIII and anti-MAP2 antibodies. The expressions of tubulin βIII and MAP2 increased significantly from the third day after treatment with TMP (Fig. 3A–E). In contrast, relatively few and short neurites were observed in control cells following the time course of DMSO treatment.

It was also noted that neuronal differentiation of the cells was accompanied by increased expression of TopoIIβ (Fig. 4D–E). Intriguingly, when we examined TopoIIα expression in comparison with TopoIIβ, we found that TopoIIα was abundantly expressed in the proliferating cells, while TopoIIβ was evidently enriched in differentiated cells (Fig. 4D–F). These results suggest that the expression pattern alters from TopoIIα to TopoIIβ in cells following differentiation.

To verify whether TMP-induced neuronal differentiation in SH-SY5Y cells was associated with TopoIIβ expression, we used ICRF-193, bis (2,6-dioxopiperazine), a topoisomerase II catalytic inhibitor (Nur-E-Kamal et al., 2007; Xiao et al., 2003), to treat the cells prior to TMP induction. Results revealed that ICRF-193 significantly decreased the average neurite length and the percentage of neurite-bearing cells (Fig. 5A–C). ICRF-193 inhibited the expression of TMP-induced neuronal marker MAP2, as revealed by Western blot assay (Fig. 5D and E). Collectively, the data indicate that TopoIIβ plays an essential role in TMP-induced neuronal differentiation of SH-SY5Y cells.

3.4. TMP-induced neuronal differentiation were regulated by PI3K/Akt, but not ERK1/2

To determine whether the critical PI3K/Akt and ERK1/2 signaling pathways are responsible for TMP-induced neuronal differentiation, we measured the phosphorylation levels of Akt and ERK1/2 with Western blot analysis. Results showed that TMP (80 μM) significantly increased the phosphorylated Akt (p-Akt, Ser473) level in the differentiated cells in a time-dependent manner (Fig. 4A and B). This differentiation could be inhibited by treatment with PI3K inhibitor LY294002, which reduced the neurite length and number of neurite-bearing cells (Fig. 6A–C). Similarly, neuronal marker expression was also reduced by LY294002 treatment (Fig. 6D, E and H). However, TMP did not obviously change the level of phosphorylated ERK1/2 (p-ERK1/2) at the observed time points in SH-SY5Y cells (Fig. 4A and C). U0126, a specific MEK1/2 inhibitor, seemed to have no effect on the differentiation process in SH-SY5Y cells (Fig. 6A–C and F–H). Therefore, we conclude that PI3K/Akt, but not ERK1/2, is activated to mediate TMP-induced neuronal differentiation of SH-SY5Y cells.

3.5. Phosphorylation of PI3K/Akt positively correlated with expression levels of Sp1 and TopoIIβ in differentiated SH-SY5Y cells

To investigate the relationship between the signaling pathways and the transcriptional factors Sp1 and NF-Y in mediating TopoIIβ expression, we measured each of their expressions in the process of neuronal differentiation. As shown in Figs. 4 and 7, Sp1 was highly expressed in differentiated cells, displaying a positive correlation with the phosphorylation of PI3K/Akt and the expression levels of TopoIIβ. This interaction was reduced by the specific inhibitor LY294002. Unlike Sp1, NF-Y is a heteromeric transcription factor, which is made up of three subunits, NF-YA, NF-YB and NF-YC (Mantovani, 1998). NF-YA is the regulatory subunit and is responsible for sequence-specific DNA binding (Manni et al., 2008). It is often used to study the role of NF-Y in regulating the expression of relevant genes (Hughes et al., 2011; Silvestre-Roig et al., 2013). Therefore, antibodies specific to the NF-YA subunit were used in this study to determine the ability of NF-Y to bind to the TopoIIβ gene promoter. It was found that the amount of NF-YA protein did not detectably change, and there was no positive correlation with PI3K/Akt and/or TopoIIβ in the differentiated SH-SY5Y cells (Figs. 4 and 7). Thus, these results indicate that the Akt/Sp1/TopoIIβ pathway may participate in TMP-induced neuronal differentiation.

We then focused on whether PI3K/Akt regulates TopoIIβ expression at a transcriptional or a translational level. We found that inhibition of PI3K/Akt by LY294002 led to decreased TopoIIβ mRNA levels in a time-dependent manner (Fig. 8A–D). The influence of the TMP-activated PI3K/Akt pathway on TopoIIβ protein biosynthesis was also considered. The effects of CHX (an inhibitor of protein biosynthesis) or α-amanitin (an RNA polymerase II inhibitor) on cells with or without TMP treatment were measured. Results showed that in TMP-treated cells, the mRNA expression of TopoIIβ was affected by α-amanitin, but not by CHX (Fig. 8E and F). Taken together, these data indicate that TMP-activated PI3K/Akt may regulate TopoIIβ gene expression at the transcriptional level, but not at the translational level.

3.6. TMP-activated PI3K/Akt increases the expression of TopoIIβ through recruitment of Sp1 to its binding site (GC-box) on the gene promoter

It is reported that activated PI3K/Akt can translocate Sp1 from the cytoplasm to the nucleus and that nuclear Sp1 binds to related gene promoters to up-regulate gene transcription. It has also been found that the PI3K/Akt inhibitor, LY294002, blocks Sp1 translocation from cytoplasm to nucleus, suggesting the activation of Sp1 by the PI3K/Akt pathway (Mireuta et al., 2010; Takao et al., 2012). Therefore, in the present study, we examined whether this regulatory role exists in the transcription of TopoIIβ, which is upregulated by the TMP-activated PI3K/Akt pathway via Sp1. We performed ChIP assays to detect the association of Sp1 to its binding site GC-box in the TopoIIβ promoter region. We found that

100 cells were counted in each medium condition. The data are expressed as the mean ± SD of three independent experiments. The asterisk represents statistically different from the corresponding control values (*$P < 0.05$ vs. control, **$P < 0.01$ vs. control, #$P < 0.05$ vs. TMP treated cells without LY294002). (D, E) PI3K/Akt inhibitor LY294002 decreased TMP-induced MAP2 expression in SH-SY5Y cells. SH-SY5Y cells were cultured in the presence or absence of 80 μM TMP for up to 5 days, the cells were lysed, and analyzed by immunoblot for MAP2 protein. The blot is representative of at least three experiments. Densitometric analysis of bands representing means ± SD of three independent experiments. Densitometry indicated TMP increased MAP2 and decrease by LY294002 in cells cultured in the presence of TMP. β-Actin was used as loading control. Error bars indicate the standard deviation of the mean. The asterisk represents statistically different from the corresponding control values (**$P < 0.01$ vs. control, #$P < 0.05$ vs. TMP treated cells without LY294002). (F, G) Effect of MEK1/2 inhibitor U0126 on TMP-induced MAP2 expression in SH-SY5Y cells. Cells were induced by 80 μM TMP in the presence or absence U0126 for up to 5 days, the cells were lysed, and analyzed by immunoblot for MAP2 protein. The blot is representative of at least three experiments. Densitometric analysis of bands representing means ± SD of three independent experiments. Densitometry indicated TMP increased MAP2 and in cells cultured in the presence of TMP. β-Actin was used as loading control. Error bars indicate the standard deviation of the mean. The asterisk represents statistically different from the corresponding control values (**$P < 0.01$ vs. control). (H) Immunofluorescent staining for neuronal marker MAP2 (red) expression in SH-SY5Y cells after 5 days differentiation by TMP with or without inhibitors (LY294002 or U0126). Scale bar = 50 μm. (For interpretation of the references to color in this figure legend, the reader is referred to the web version of this article.)

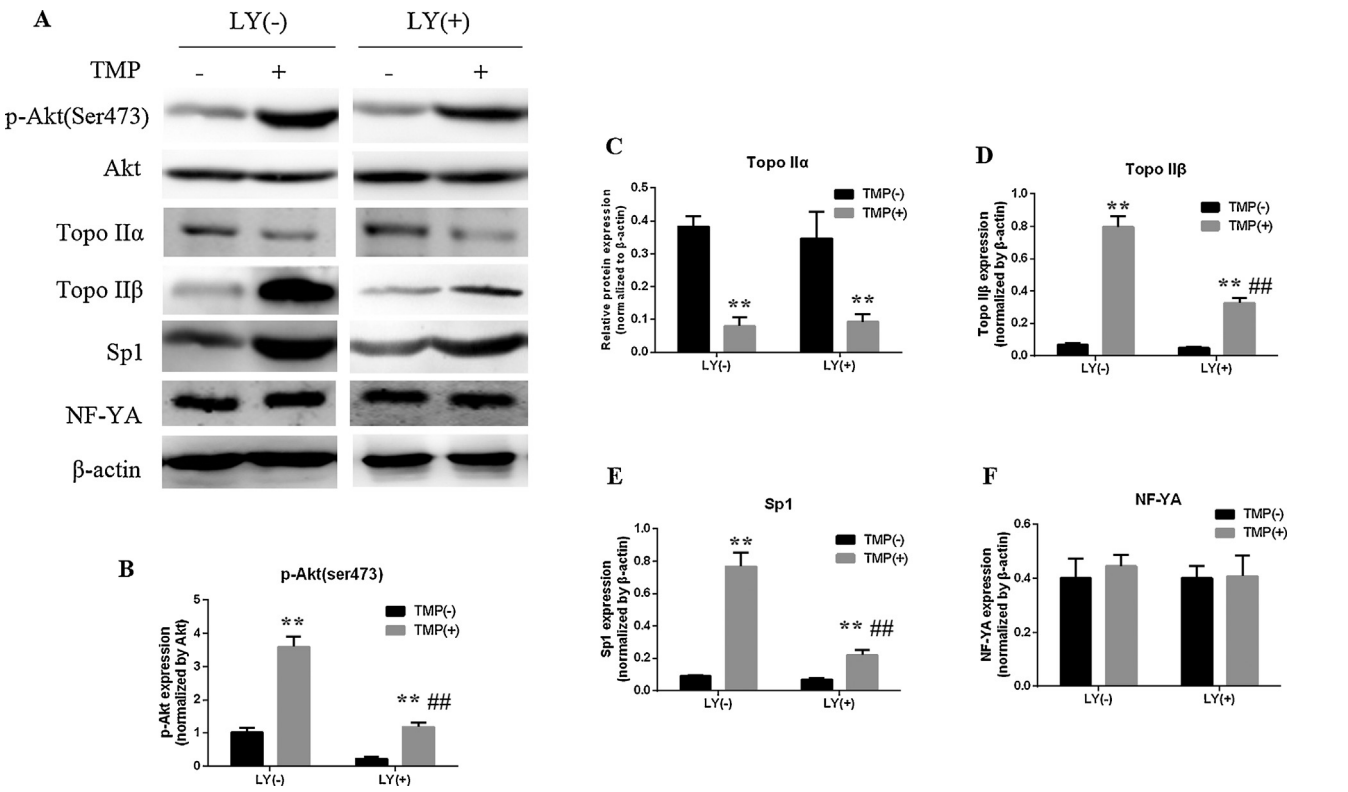

Fig. 7. LY294002 inhibited the expression of Sp1 and TopoIIβ. (A) Representative immunoblots of at least three experiments. Western blots show the expression of p-Akt, TopoIIα, TopoIIβ, Sp1 and NF-YA proteins during treatment with 80 μM TMP with or without LY294002 for 5 days. Akt was used for p-Akt and β-actin was used for other proteins respectively as a control for normalizing the optical density of each band. (B–F) Densitometric analysis of bands representing means ± SD of three independent experiments. The ratios of p-Akt to Akt, while TopoIIα, TopoIIβ, Sp1 and NF-YA proteins to β-actin were quantified respectively. Densitometry indicated that increased expression of p-Akt, TopoIIβ and Sp1 were inhibited by LY294002 in the cells treated with TMP. The decreased TopoIIα and unchanged NF-YA expression after TMP treatment were both not affected by LY294002. Error bars indicate the standard deviation of the mean. The asterisk represents statistically different from the corresponding control values (**$P < 0.01$ vs. control, ##$P < 0.01$ vs. TMP-treated cells without LY294002).

the association of Sp1 with the TopoIIβ promoter was enhanced in cells after 1 day of TMP treatment, and was inhibited by the specific PI3K/Akt inhibitor LY294002 (Fig. 9A, B and D). The data support the theory that the PI3K/Akt signal enhances Sp1 translocation from cytoplasm to nucleus, where it binds to TopoIIβ promoters and upregulates gene expression in the early stages of neuronal differentiation in SH-SY5Y cells induced by TMP.

Another transcription factor, NF-Y, was also reported to be critical for TopoIIβ transcription, acting by binding to the inverted CCAAT boxes on the gene promoter (Lok et al., 2002). To examine its role in the transcriptional activation of TopoIIβ in neuronally differentiated cells, we investigated the association of one of its subunits, NF-YA, with the TopoIIβ gene promoter region using ChIP assays. Compared to Sp1, cells at the initial stage of differentiation exhibited no detectable NF-Y DNA-binding activity, but the binding progressively increased from the third day after TMP treatment (Fig. 9A, C and D). However, NF-YA recruitment to the TopoIIβ promoter was not diminished by the PI3K/Akt inhibitor LY294002. These results suggest that NF-Y possibly regulates TopoIIβ at later stages of differentiation, independently from the PI3K/Akt signaling pathway.

4. Discussion

Neural differentiation, controlled by appropriate regulation of extrinsic signaling factors and intrinsic cell-specific genes, is relevant to a wide range of biological events in the nervous system, including neural development, neurological damage and repair (Christie and Turnley, 2012), neurodegenerative disorders (Ziemka-Nalecz and Zalewska, 2012), and the formation and treatment of nervous system neoplasms (Han et al., 2014). Neuronal differentiation is extremely complicated because it can occur in different cell types and be caused by a variety of inducers (Kong et al., 2015; Tian et al., 2010; Xiao et al., 2010; Yu et al., 2009). In recent years, considerable attention has been paid to the identification of new differentiation-related genes, proteins and signaling pathways to gain insights into the mechanisms involved in differentiation and possible treatments of neurobiological disorders (Lee et al., 2009; Lim et al., 2008).

Drugs that can protect neurons or increase neurogenesis from neural stem cells/neural progenitor cells, both in vitro and in vivo, hold promise for the treatment of nervous system disorders, including neurodegenerative diseases. Currently, numerous compounds have been shown to play a role in the biological processes of neuronal differentiation, and that raises the possibility of curing neuron injury and/or neurodegenerative diseases. For example, sodium butyrate, a naturally occurring short-chain fatty acid, markedly expands the population of proliferating cells in the ipsilateral ischemic brain hemisphere of rats that have undergone permanent middle cerebral artery occlusion (Kim et al., 2009). Valproic acid, a well-known anticonvulsant and mood stabilizer, promotes neuronal differentiation through the induction of pro-neural factors, such as Ngn1, Math1 and p15, by enhancing the association of acetylated histone H4 to their promoter regions (Yu et al., 2009). All-trans-retinoic acid, an essential factor derived from vitamin A, appears to act on a wide variety of pathways and mechanisms that are affected in Alzheimer's disease (Lee et al., 2009). Kuwanon V, which is isolated from the mulberry tree (*Morus bombycis*) root, increases neurogenesis and differentiation in rat neural stem cells (Kong et al., 2015). TMP, one of the natural alkaloids isolated from

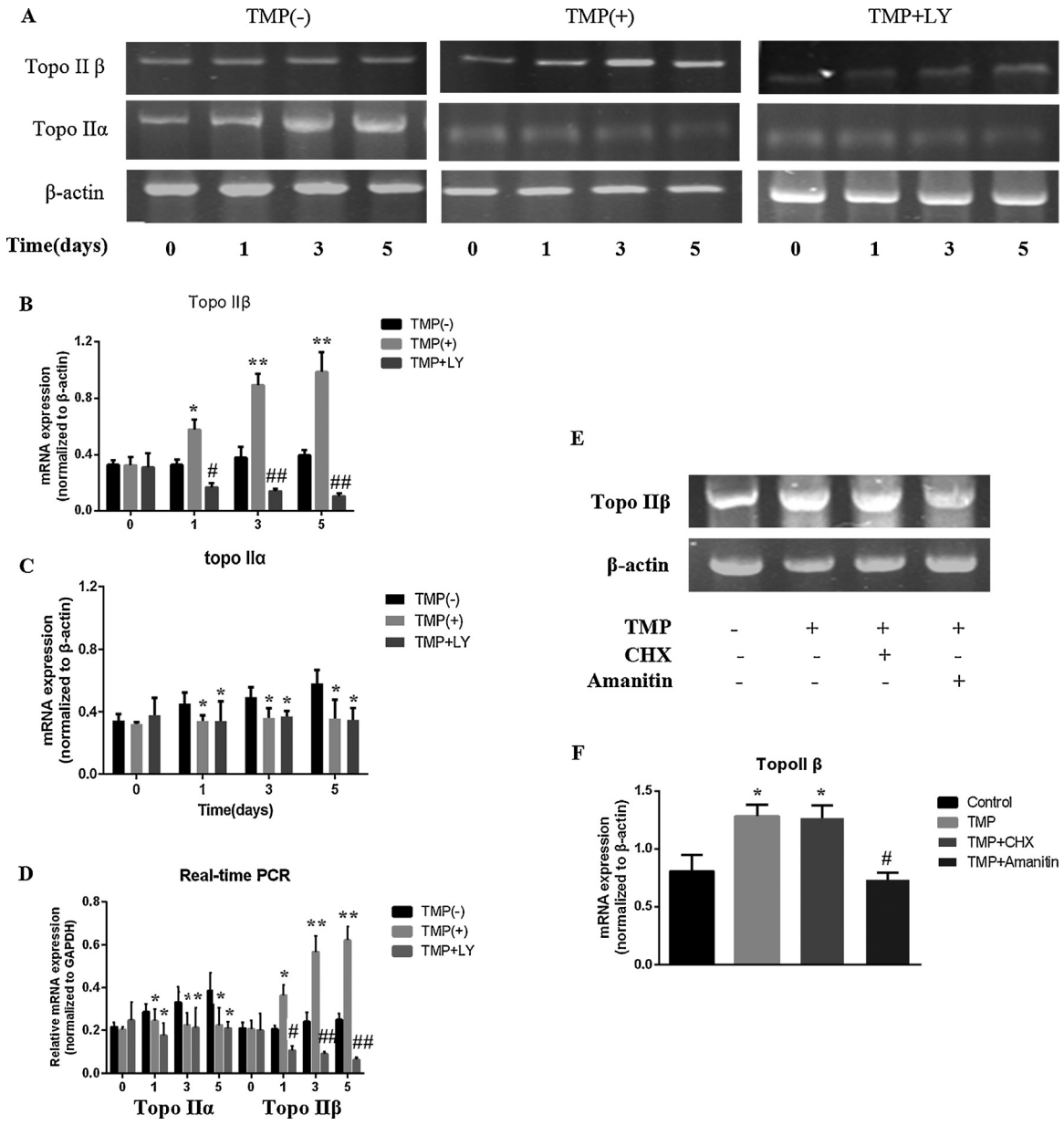

Fig. 8. LY294002 attenuated the upregulation of TopIIβ upon TMP treatment at transcriptional level. (A–C) The mRNA expression of TopoIIα and TopoIIβ detected by semi-quantity RT-PCR. SH-SY5Y cells were treated with TMP in the absence or presence of LY294002 for indicated days. The total RNA was extracted for TopoIIα and TopoIIβ mRNA detection. Shown are representative bands of at least three experiments. Densitometric analysis of bands representing means ± SD of three independent experiments. Densitometry indicated increase of TopoIIβ in cells cultured in the presence of TMP. LY294002 repressed the TMP induced TopoIIβ mRNA expression. β-Actin was used as loading control. Error bars indicate the standard deviation of the mean. The asterisk represents statistically different from the corresponding control values ($^{*}P < 0.05$ vs. control, $^{**}P < 0.01$ vs. control, $^{\#}P < 0.05$ vs. TMP-treated cells without LY294002, $^{\#\#}P < 0.01$ vs. TMP-treated cells without LY294002). (D) Real-time quantitative PCR (RT-qPCR) examined the TopoIIα and TopoIIβ mRNA expression. The asterisk represents statistically different from the corresponding control values ($^{*}P < 0.05$ vs. control, $^{**}P < 0.01$ vs. control, $^{\#}P < 0.05$ vs. TMP-treated cells without LY294002, $^{\#\#}P < 0.01$ vs. TMP-treated cells without LY294002). (E, F) Cells were stimulated with α-amanitin (50 μg/mL) or CHX (10 mM) in the absence or presence of TMP for 5 days, then total RNA was extracted for TopoIIβ detection. β-Actin was treated as internal control. All results are means ± SD of three independent experiments. Error bars indicate the standard deviation of the mean. The asterisk represents statistically different from the corresponding control values ($^{*}P < 0.05$ vs. control, $^{\#}P < 0.05$ vs. TMP-treated cells).

the Chinese herb Chuanxiong, has been shown to promote neuronal differentiation of neural stem cells (Tian et al., 2010; Xiao et al., 2010), and in the present study we focused on its role in promoting neuronal differentiation by targeting TopoIIβ, and on unraveling the underlying mechanism.

Given that the transcription of the TopoIIβ gene is regulated mainly by a region between −553 and −481 relative to the transcription start site, with binding sites for Sp1 and NF-Y at the gene promoter (Lok et al., 2002), and that Sp1 plays an important role in regulation of TopoIIβ during neuronal differentiation (Guo et al., 2014) in addition to Sp1 and NF-Y being the downstream effectors of ERK 1/2 and Akt signaling cascades (Chang et al., 2013; Takao et al., 2012; Vasilaki et al., 2010), we hypothesized that these components may provide targets for TMP's promotion of neuronal differentiation.

Firstly, our results showed that 80 μM TMP induced SH-SY5Y cells to form a neuronal cell type characterized by increased neuronal markers and neurite outgrowth without compromising cell survival. In addition, the expression of TopoIIβ protein was up-regulated during the neuronal differentiation process. Blocking TopoIIβ with ICRF-193 resulted in reduced TopoIIβ expression and repressed the neuronal differentiation. Further

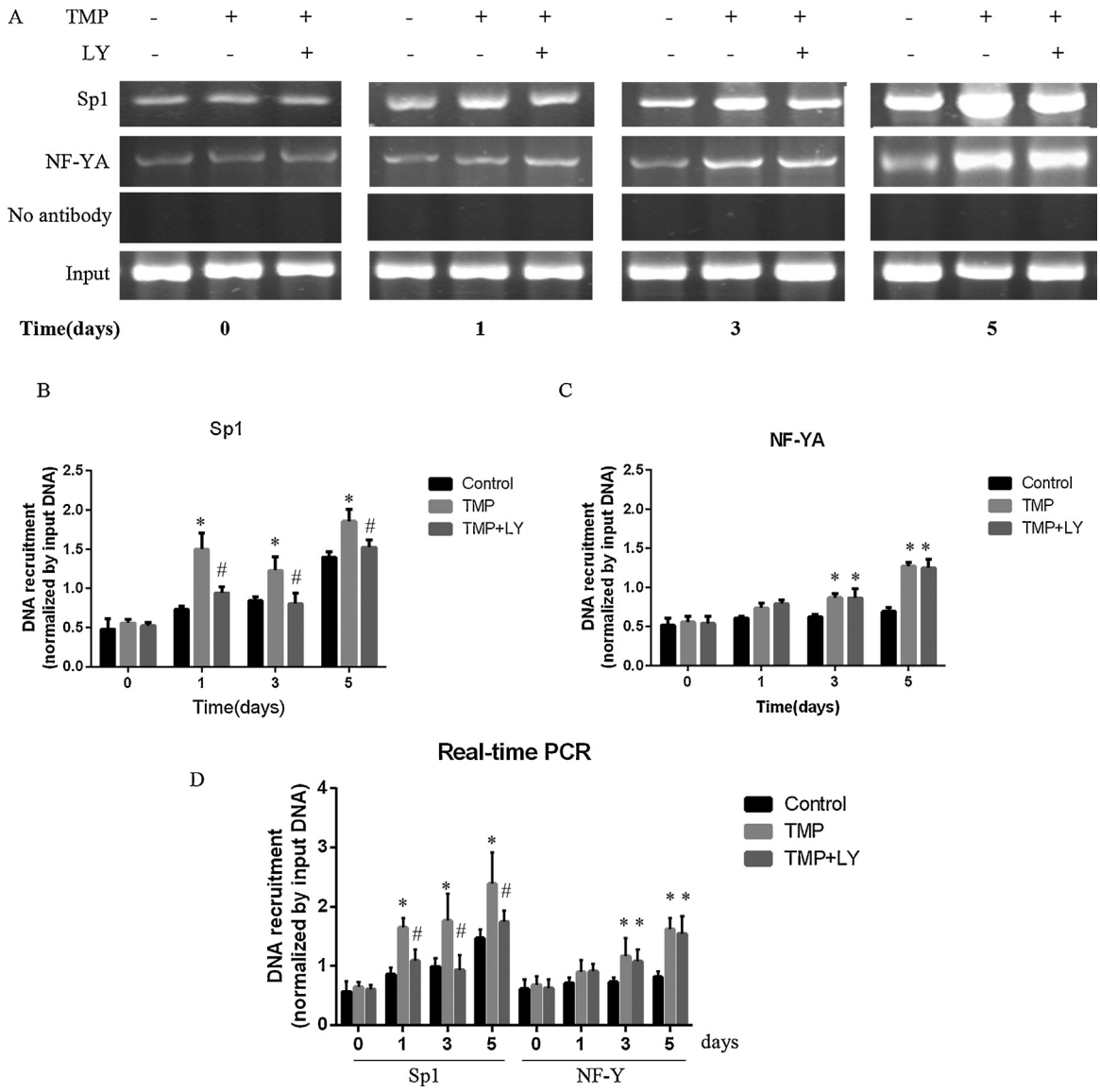

Fig. 9. ChIP analysis of Sp1 and NF-YA on proximal region of TopoIIβ promoter in response to TMP with or without LY294002 in SH-SY5Y cell line. Chromatin was cross-linked, prepared, digested, and immunoprecipitated with anti-Sp1 or NF-YA antibodies. In order to analyze for the presence of TopoIIβ promoter sequence, aliquots of and dilutions of non-precipitated (Input) DNA were submitted to PCR amplification using specific primers: a primer pair spanning 700 bp on proximal region of TopoIIβ promoter (between 599 bp upstream and 100 bp downstream relative to transcription start site (TSS)). In addition to immunoprecipitated and input DNA, DNA collected from samples with no antibody was also amplified as negative controls and performed on aliquots from the same chromatin preparation. (A) Twenty percent of each amplification reaction was electrophoresed in a 1.5% agarose gel and visualized by GoldView nucleic acid dye. A representative gels were shown for the binding of Sp1 or NF-YA to TopoIIβ promoter region. (B–D) The relative levels of the binding of Sp1 or NF-YA to TopoIIβ promoter region were calculated and normalized to the input DNA. Real-time quantitative PCR (RT-qPCR) results of immunoprecipitated DNA for confirmation are shown in (D). Results are the mean ± SD for three amplifications of three independent precipitations. Error bars indicate the standard deviation (SD) of the mean. The asterisk represents statistically different from the corresponding control values ($^{*}P < 0.05$ vs. control, $^{\#}P < 0.05$ vs. TMP-treated cells without LY294002).

investigation using an RNA polymerase II inhibitor, α-amanitin, indicated that TMP promotes TopoIIβ expression at the transcription level. Interestingly, the other topoisomerase isoform, TopoIIα, was down-regulated following TMP treatment. Such alterations coincide with the findings of other studies, which describe a molecular switch from TopoIIα to TopoIIβ during neural differentiation in mouse embryonic stem cells (Tiwari et al., 2012), and in bone marrow-derived human mesenchymal stem cells (Isik et al., 2015), which may reflect changes in the expression of specific neuronal genes in cells undergoing postmitotic terminal differentiation.

Next, we ascertained whether related cell signaling pathways were involved in this process. It is well known that ERK 1/2 and/or PI3K/Akt signaling pathways are pivotal for neuronal differentiation in a number of cell types (Lopez-Carballo et al., 2002; Tsao et al., 2013). In the process of differentiation, PI3K/Akt and ERK pathways can act independently or cooperatively (Lim et al., 2008; Tsao et al., 2013). Previous reports have shown that the PI3K/Akt pathway is required for retinoic acid-induced neuroblastoma cell differentiation (Lopez-Carballo et al., 2002; Qiao et al., 2012), while other research indicates a positive relationship between the phosphorylation of ERK1/2 and differentiation of rat neural stem cells after TMP treatment (Tian et al., 2010). It has also been found that the activation of ERK1/2 is necessary for directing adult spinal cord endogenous neural stem/progenitor cells toward a neuronal fate (Chan et al., 2013). In this study, we assessed the contribution of these pathways to neuronal differentiation in SH-SY5Y cells. We found that TMP induced the activation of PI3K/Akt, but not ERK 1/2. Moreover, PI3K/Akt positively correlated with the expression

of TopoIIβ mRNA and protein in the differentiated neuron-like cells. Inhibition of the PI3K/Akt pathway by the chemical inhibitor LY294002 not only decreased the expression of TopoIIβ, but also disrupted the neuronal differentiation of SH-SY5Y cells. These results confirm that PI3K/Akt is involved in the neuronal differentiation induced by TMP. It suggests that which signal, ERK1/2 or PI3K/Akt, promotes neuronal differentiation may be cell type-specific or agent-dependent.

We also assessed whether Sp1 and/or NF-Y were the downstream targets of PI3K/Akt in mediating TopoIIβ expression. Sp1 is a sequence-specific transcription factor that recognizes GGGGCGGGGC and closely related sequences, which are often referred to as GC boxes or GC islands, and is positively related to neuronal differentiation in various cell types through its action on a number of genes (Gong et al., 2014; Paonessa et al., 2013). Sp1 can be regulated by the PI3K/Akt signaling cascade (Hong et al., 2014; Takao et al., 2012). It has been demonstrated that TopoIIβ is transcriptionally regulated by Sp1-responsive elements within the GC island in the TopoIIβ promoter (Lok et al., 2002). In this study, we performed Western blot and ChIP assay to determine the relationship between Sp1 and PI3K/Akt during TMP-induced neuronal differentiation of SH-SY5Y cells. Results showed that Sp1 expression level and its recruitment to the TopoIIβ core promoter region are positively correlated to the phosphorylation of Akt. These results established a tight relationship between the PI3K/Akt/Sp1 signaling pathway and TopoIIβ expression in TMP-induced neuronally differentiated SH-SY5Y cells.

NF-Y is another transcriptional factor, which binds to the CCAAT boxes on the TopoIIβ gene promoter (Lok et al., 2002). It is often pivotal in cell models of the differentiation process (Chen et al., 2008; Ly et al., 2013; Yoshioka et al., 2012). Also, NF-Y has been identified as an important downstream mediator in the ERK 1/2 and Akt-dependent signaling cascades that contribute to regulating certain cellular gene (Silvestre-Roig et al., 2013). Compared to Sp1, there is little published research regarding NF-Y's roles in neuronal differentiation. One study has demonstrated that NF-Y is active in mature, differentiated neurons, and conditional deletion of the subunit NF-YA in postmitotic mouse neurons induces progressive neurodegeneration (Yamanaka et al., 2014). In contrast, other reports indicate that NF-YA, NF-YB and NF-YC transcripts display relatively constant steady state levels, with little variation in differentiating neurons (Piens et al., 2010). In this study, we showed that the level of NF-YA did not significantly change during the entire differentiation procedure after TMP treatment. On the contrary, it became apparently sensitive and was recruited to its binding sites on the TopoIIβ promoter after 3 days of TMP treatment, which is not affected by PI3K/Akt pathway. This different regulation of Sp1 and NF-Y by PI3K/Akt after TMP treatment has been unclear until now. It appears that other mechanisms may be involved in the differentiation program in addition to the PI3K/Akt and ERK1/2 signaling pathways. For example, it may be caused by an open chromatin state resulting from the acetylation of histones H3 and H4 at the TopoIIβ gene promoter as reported in our previous study (Yan et al., 2014). These epigenetic alterations to the TopoIIβ gene structure may lead to increased NF-Y and Sp1 affinity for the TopoIIβ gene promoter, resulting in increased TopoIIβ expression and the promotion of neuronal differentiation.

In summary, neuronal differentiation is a complex process involving the coordinated activity of numerous signaling pathways. In this study we explored the modulatory effects of TMP on TopoIIβ via some of these pathways in the context of the SH-SY5Y cell model. We found that Sp1 and TopoIIβ expression are tightly correlated with the PI3K/Akt signaling cascade. On the other hand, the involvement of NF-Y in TopoIIβ modulation is independent of both PI3K/Akt and ERK1/2 signals, but may be affected by the chromatin state of the gene. These results suggest wide molecular and functional diversity in controlling neural differentiation in response to different chemical inducers.

5. Conclusions

We have shown that TMP induces differentiation of SH-SY5Y cells to a neuronal phenotype as a result of up-regulation of TopoIIβ via the PI3K/Akt/Sp1 signaling pathway. Our study provides novel perspectives and potential targets for TMP's promotion of neuronal differentiation. These results highlight the role of TopoIIβ in neuronal differentiation. Data from this study suggest the potential use of TMP in chemical therapies for neurodegenerative diseases and neuronal injuries. Further studies should focus on other related downstream targets of TMP that are essential for neural differentiation, and work is also required to analyze the role of TMP in neurogenesis in vivo.

6. Competing interests

The authors declare that there are no competing interests. All authors have read and approved the final manuscript.

7. Authors' contributions

Yongxin Yan conceived and designed experiments, performed the experiments, drafted the article, and prepared the digital images. Yunli Yan designed experiments and drafted the article. Junxia Zhao, Shengjie Yao and Zhiqiang Jia supplied the SH-SY5Y cell, performed the MTT assay and proofread the manuscript. Najing Zhou performed part of the Western blot assays and provided limited financial support. Yanling Wang, Yannan Xu and Junan Zhao supplied technological support during cell culture and reagents preparation. Cuili Cao and Shuo Han captured the images of the cultured cell, counted the neurite length and help to analyze the data. Shuo Han supplied technological support during the PCR performance. Huixia Cui has given constructive suggestions to improve this work.

References

Agholme, L., Lindstrom, T., Kagedal, K., Marcusson, J., Hallbeck, M., 2010. An in vitro model for neuroscience: differentiation of SH-SY5Y cells into cells with morphological and biochemical characteristics of mature neurons. J. Alzheimer's Dis. 20, 1069–1082.

Anderton, R.S., Meloni, B.P., Mastaglia, F.L., Greene, W.K., Boulos, S., 2011. Survival of motor neuron protein over-expression prevents calpain-mediated cleavage and activation of procaspase-3 in differentiated human SH-SY5Y cells. Neuroscience 181, 226–233.

Austin, C.A., Marsh, K.L., 1998. Eukaryotic DNA topoisomerase II beta. BioEssays 20, 215–226.

Chan, W.S., Sideris, A., Sutachan, J.J., Montoya, G.J., Blanck, T.J., Recio-Pinto, E., 2013. Differential regulation of proliferation and neuronal differentiation in adult rat spinal cord neural stem/progenitors by ERK1/2, Akt, and PLCgamma. Front. Mol. Neurosci. 6, 23.

Chang, K.W., Huang, Y.L., Wong, Z.R., Su, P.H., Huang, B.M., Ju, T.K., Yang, H.Y., 2013. Fibroblast growth factor-2 up-regulates the expression of nestin through the Ras-Raf-ERK-Sp1 signaling axis in C6 glioma cells. Biochem. Biophys. Res. Commun. 434, 854–860.

Chen, S., Gluhak-Heinrich, J., Martinez, M., Li, T., Wu, Y., Chuang, H.H., Chen, L., Dong, J., Gay, I., MacDougall, M., 2008. Bone morphogenetic protein 2 mediates dentin sialophosphoprotein expression and odontoblast differentiation via NF-Y signaling. J. Biol. Chem. 283, 19359–19370.

Chen, Z., Pan, X., Georgakilas, A.G., Chen, P., Hu, H., Yang, Y., Tian, S., Xia, L., Zhang, J., Cai, X., Ge, J., Yu, K., Zhuang, J., 2013. Tetramethylpyrazine (TMP) protects cerebral neurocytes and inhibits glioma by down regulating chemokine receptor CXCR4 expression. Cancer Lett. 336, 281–289.

Christie, K.J., Turnley, A.M., 2012. Regulation of endogenous neural stem/progenitor cells for neural repair-factors that promote neurogenesis and gliogenesis in the normal and damaged brain. Front. Cell. Neurosci. 6, 70.

Ding, Y., Hou, X., Chen, L., Li, H., Tang, Y., Zhou, H., Zhao, S., Zheng, Y., 2013. Protective action of tetramethylpyrazine on the medulla oblongata in rats with chronic hypoxia. Auton. Neurosci. Basic Clin. 173, 45–52.

Dore, J.J., DeWitt, J.C., Setty, N., Donald, M.D., Joo, E., Chesarone, M.A., Birren, S.J., 2009. Multiple signaling pathways converge to regulate bone-morphogenetic-protein-dependent glial gene expression. Dev. Neurosci. 31, 473–486.
Forterre, P., Gribaldo, S., Gadelle, D., Serre, M.-C., 2007. Origin and evolution of DNA topoisomerases. Biochimie 89, 427–446.
Fu, Y.S., Lin, Y.Y., Chou, S.C., Tsai, T.H., Kao, L.S., Hsu, S.Y., Cheng, F.C., Shih, Y.H., Cheng, H., Fu, Y.Y., Wang, J.Y., 2008. Tetramethylpyrazine inhibits activities of glioma cells and glutamate neuro-excitotoxicity: potential therapeutic application for treatment of gliomas. Neuro-Oncology 10, 139–152.
Gong, L., Ji, W.K., Hu, X.H., Hu, W.F., Tang, X.C., Huang, Z.X., Li, L., Liu, M., Xiang, S.H., Wu, E., Woodward, Z., Liu, Y.Z., Nguyen, Q.D., Li, D.W., 2014. Sumoylation differentially regulates Sp1 to control cell differentiation. Proc. Natl. Acad. Sci. U. S. A. 111, 5574–5579.
Guo, H., Cao, C., Chi, X., Zhao, J., Liu, X., Zhou, N., Han, S., Yan, Y., Wang, Y., Xu, Y., Yan, Y., Cui, H., Sun, H., 2014. Specificity protein 1 regulates topoisomerase IIbeta expression in SH-SY5Y cells during neuronal differentiation. J. Neurosci. Res. 92, 1374–1383.
Han, X., Gui, B., Xiong, C., Zhao, L., Liang, J., Sun, L., Yang, X., Yu, W., Si, W., Yan, R., Yi, X., Zhang, D., Li, W., Li, L., Yang, J., Wang, Y., Sun, Y.E., Zhang, D., Meng, A., Shang, Y., 2014. Destabilizing LSD1 by Jade-2 promotes neurogenesis: an antibraking system in neural development. Mol. Cell 55, 482–494.
Heng, X., Le, W.D., 2010. The function of DNA topoisomerase IIbeta in neuronal development. Neurosci. Bull. 26, 411–416.
Hong, I.K., Byun, H.J., Lee, J., Jin, Y.J., Wang, S.J., Jeoung, D.I., Kim, Y.M., Lee, H., 2014. The tetraspanin CD81 protein increases melanoma cell motility by up-regulating metalloproteinase MT1-MMP expression through the pro-oncogenic Akt-dependent Sp1 activation signaling pathways. J. Biol. Chem. 289, 15691–15704.
Hu, J.Z., Huang, J.H., Xiao, Z.M., Li, J.H., Li, X.M., Lu, H.B., 2013. Tetramethylpyrazine accelerates the function recovery of traumatic spinal cord in rat model by attenuating inflammation. J. Neurol. Sci. 324, 94–99.
Hughes, R., Kristiansen, M., Lassot, I., Desagher, S., Mantovani, R., Ham, J., 2011. NF-Y is essential for expression of the proapoptotic bim gene in sympathetic neurons. Cell Death Differ. 18, 937–947.
Isik, S., Zaim, M., Yildiz, M.T., Negis, Y., Kunduraci, T., Karakas, N., Arikan, G., Cetin, G., 2015. DNA topoisomerase IIbeta as a molecular switch in neural differentiation of mesenchymal stem cells. Ann. Hematol. 94, 307–318.
Kim, H.J., Leeds, P., Chuang, D.M., 2009. The HDAC inhibitor, sodium butyrate, stimulates neurogenesis in the ischemic brain. J. Neurochem. 110, 1226–1240.
Kong, S.Y., Park, M.H., Lee, M., Kim, J.O., Lee, H.R., Han, B.W., Svendsen, C.N., Sung, S.H., Kim, H.J., 2015. Kuwanon v inhibits proliferation, promotes cell survival and increases neurogenesis of neural stem cells. PLOS ONE 10, e0118188.
Kurauchi, Y., Hisatsune, A., Isohama, Y., Sawa, T., Akaike, T., Shudo, K., Katsuki, H., 2011. Retinoic acid receptor-regulated NO/cyclic GMP signaling pathway promotes S-guanylation of β-tubulin and activation of MEK/ERK signaling pathway resulting in neurite differentiation in SH-SY5Y neuroblastoma cells. Neurosci. Res. 71 (Suppl.), e115.
Lee, H.P., Casadesus, G., Zhu, X., Lee, H.G., Perry, G., Smith, M.A., Gustaw-Rothenberg, K., Lerner, A., 2009. All-trans retinoic acid as a novel therapeutic strategy for Alzheimer's disease. Expert Rev. Neurother. 9, 1615–1621.
Lim, J.Y., Park, S.I., Oh, J.H., Kim, S.M., Jeong, C.H., Jun, J.A., Lee, K.S., Oh, W., Lee, J.K., Jeun, S.S., 2008. Brain-derived neurotrophic factor stimulates the neural differentiation of human umbilical cord blood-derived mesenchymal stem cells and survival of differentiated cells through MAPK/ERK and PI3K/Akt-dependent signaling pathways. J. Neurosci. Res. 86, 2168–2178.
Lok, C.N., Lang, A.J., Mirski, S.E.L., Cole, S.P.C., 2002. Characterization of the human topoisomerase IIbeta (TOP2B) promoter activity: essential roles of the nuclear factor-Y (NF-Y)- and specificity protein-1 (Sp1)-binding sites. Biochem. J. 368, 741–751.
Lopez-Carballo, G., Moreno, L., Masia, S., Perez, P., Barettino, D., 2002. Activation of the phosphatidylinositol 3-kinase/Akt signaling pathway by retinoic acid is required for neural differentiation of SH-SY5Y human neuroblastoma cells. J. Biol. Chem. 277, 25297–25304.
Lv, L., Meng, Q., Xu, J., Gong, J., Cheng, Y., Jiang, S., 2012. Ligustrazine attenuates myocardial ischemia reperfusion injury in rats by activating the phosphatidylinositol 3-kinase/Akt pathway. Ann. Clin. Lab. Sci. 42, 198–202.
Ly, L.L., Suyari, O., Yoshioka, Y., Tue, N.T., Yoshida, H., Yamaguchi, M., 2013. dNF-YB plays dual roles in cell death and cell differentiation during Drosophila eye development. Gene 520, 106–118.
Lyu, Y.L., Lin, C.P., Azarova, A.M., Cai, L., Wang, J.C., Liu, L.F., 2006. Role of topoisomerase IIbeta in the expression of developmentally regulated genes. Mol. Cell. Biol. 26, 7929–7941.
Manni, I., Caretti, G., Artuso, S., Gurtner, A., Emiliozzi, V., Sacchi, A., Mantovani, R., Piaggio, G., 2008. Posttranslational regulation of NF-YA modulates NF-Y transcriptional activity. Mol. Biol. Cell 19, 5203–5213.
Mantovani, R., 1998. A survey of 178 NF-Y binding CCAAT boxes. Nucleic Acids Res. 26, 1135–1143.
Mireuta, M., Darnel, A., Pollak, M., 2010. IGFBP-2 expression in MCF-7 cells is regulated by the PI3K/AKT/mTOR pathway through Sp1-induced increase in transcription. Growth Factors 28, 243–255.
Nur-E-Kamal, A., Meiners, S., Ahmed, I., Azarova, A., Lin, C.-p., Lyu, Y.L., Liu, L.F., 2007. Role of DNA topoisomerase IIβ in neurite outgrowth. Brain Res. 1154, 50–60.
Oe, T., Sasayama, T., Nagashima, T., Muramoto, M., Yamazaki, T., Morikawa, N., Okitsu, O., Nishimura, S., Aoki, T., Katayama, Y., Kita, Y., 2005. Differences in gene expression profile among SH-SY5Y neuroblastoma subclones with different neurite outgrowth responses to nerve growth factor. J. Neurochem. 94, 1264–1276.
Pang, P.K., Shan, J.J., Chiu, K.W., 1996. Tetramethylpyrazine, a calcium antagonist. Planta Med. 62, 431–435.
Paonessa, F., Latifi, S., Scarongella, H., Cesca, F., Benfenati, F., 2013. Specificity protein 1 (Sp1)-dependent activation of the synapsin I gene (SYN1) is modulated by RE1-silencing transcription factor (REST) and 5′-cytosine-phosphoguanine (CpG) methylation. J. Biol. Chem. 288, 3227–3239.
Piens, M., Muller, M., Bodson, M., Baudouin, G., Plumier, J.C., 2010. A short upstream promoter region mediates transcriptional regulation of the mouse doublecortin gene in differentiating neurons. BMC Neurosci. 11, 64.
Qiao, J., Paul, P., Lee, S., Qiao, L., Josifi, E., Tiao, J.R., Chung, D.H., 2012. PI3K/AKT and ERK regulate retinoic acid-induced neuroblastoma cellular differentiation. Biochem. Biophys. Res. Commun. 424, 421–426.
Silvestre-Roig, C., Fernandez, P., Esteban, V., Pello, O.M., Indolfi, C., Rodriguez, C., Rodriguez-Calvo, R., Lopez-Maderuelo, M.D., Bauriedel, G., Hutter, R., Fuster, V., Ibanez, B., Redondo, J.M., Martinez-Gonzalez, J., Andres, V., 2013. Inactivation of nuclear factor-Y inhibits vascular smooth muscle cell proliferation and neointima formation. Arterioscler. Thromb. Vasc. Biol. 33, 1036–1045.
Takao, T., Asanoma, K., Tsunematsu, R., Kato, K., Wake, N., 2012. The maternally expressed gene Tssc3 regulates the expression of MASH2 transcription factor in mouse trophoblast stem cells through the AKT-Sp1 signaling pathway. J. Biol. Chem. 287, 42685–42694.
Tan, K.B., Dorman, T.E., Falls, K.M., Chung, T.D., Mirabelli, C.K., Crooke, S.T., Mao, J., 1992. Topoisomerase II alpha and topoisomerase II beta genes: characterization and mapping to human chromosomes 17 and 3, respectively. Cancer Res. 52, 231–234.
Tian, Y., Liu, Y., Chen, X., Zhang, H., Shi, Q., Zhang, J., Yang, P., 2010. Tetramethylpyrazine promotes proliferation and differentiation of neural stem cells from rat brain in hypoxic condition via mitogen-activated protein kinases pathway in vitro. Neurosci. Lett. 474, 26–31.
Tiwari, V.K., Burger, L., Nikoletopoulou, V., Deogracias, R., Thakurela, S., Wirbelauer, C., Kaut, J., Terranova, R., Hoerner, L., Mielke, C., Boege, F., Murr, R., Peters, A.H., Barde, Y.A., Schubeler, D., 2012. Target genes of topoisomerase IIbeta regulate neuronal survival and are defined by their chromatin state. Proc. Natl. Acad. Sci. U. S. A. 109, E934–E943.
Tsao, H.K., Chiu, P.H., Sun, S.H., 2013. PKC-dependent ERK phosphorylation is essential for P2X7 receptor-mediated neuronal differentiation of neural progenitor cells. Cell Death Dis. 4, e751.
Tsuda, L., Lim, Y.M., 2014. Regulatory system for the G1-arrest during neuronal development in Drosophila. Dev. Growth Differ. 56, 358–367.
Tsutsui, K., Tsutsui, K., Sano, K., Kikuchi, A., Tokunaga, A., 2001. Involvement of DNA topoisomerase IIbeta in neuronal differentiation. J. Biol. Chem. 276, 5769–5778.
Turley, H., Comley, M., Houlbrook, S., Nozaki, N., Kikuchi, A., Hickson, I.D., Gatter, K., Harris, A.L., 1997. The distribution and expression of the two isoforms of DNA topoisomerase II in normal and neoplastic human tissues. Br. J. Cancer 75, 1340–1346.
Vávrová, A., Šimůnek, T., 2012. DNA topoisomerase IIβ: a player in regulation of gene expression and cell differentiation. Int. J. Biochem. Cell Biol. 44, 834–837.
Vasilaki, E., Papadimitriou, E., Tajadura, V., Ridley, A.J., Stournaras, C., Kardassis, D., 2010. Transcriptional regulation of the small GTPase RhoB gene by TGF{beta}-induced signaling pathways. FASEB J. 24, 891–905.
Wang, J.C., 2002. Cellular roles of DNA topoisomerases: a molecular perspective. Nature Rev. Mol. Cell Biol. 3, 430–440.
Wu, W., Yu, X., Luo, X.-P., Yang, S.-H., Zheng, D., 2013. Tetramethylpyrazine protects against scopolamine-induced memory impairments in rats by reversing the cAMP/PKA/CREB pathway. Behav. Brain Res. 253, 212–216.
Xiao, H., Mao, Y., Desai, S.D., Zhou, N., Ting, C.Y., Hwang, J., Liu, L.F., 2003. The topoisomerase IIbeta circular clamp arrests transcription and signals a 26S proteasome pathway. Proc. Natl. Acad. Sci. U. S. A. 100, 3239–3244.
Xiao, X., Liu, Y., Qi, C., Qiu, F., Chen, X., Zhang, J., Yang, P., 2010. Neuroprotection and enhanced neurogenesis by tetramethylpyrazine in adult rat brain after focal ischemia. Neurol. Res. 32, 547–555.
Xu, H., Shi, D.Z., Guan, C.Y., 2003. Clinical application and pharmacological actions of ligustrazine. Chin. J. Integr. Med. 23, 376–379.
Yamanaka, T., Tosaki, A., Kurosawa, M., Matsumoto, G., Koike, M., Uchiyama, Y., Maity, S.N., Shimogori, T., Hattori, N., Nukina, N., 2014. NF-Y inactivation causes atypical neurodegeneration characterized by ubiquitin and p62 accumulation and endoplasmic reticulum disorganization. Nat. Commun. 5, 3354.
Yan, Y., Zhao, J., Cao, C., Jia, Z., Zhou, N., Han, S., Wang, Y., Xu, Y., Zhao, J., Yan, Y., Cui, H., 2014. Tetramethylpyrazine promotes SH-SY5Y cell differentiation into neurons through epigenetic regulation of topoisomerase IIbeta. Neuroscience 278, 179–193.
Yang, X., Li, W., Prescott, E.D., Burden, S.J., Wang, J.C., 2000. DNA topoisomerase IIbeta and neural development. Science 287, 131–134.
Yang, Z., Zhang, Q., Ge, J., Tan, Z., 2008. Protective effects of tetramethylpyrazine on rat retinal cell cultures. Neurochem. Int. 52, 1176–1187.
Yin, P., Zhao, C., Li, Z., Mei, C., Yao, W., Liu, Y., Li, N., Qi, J., Wang, L., Shi, Y., Qiu, S., Fan, J., Zha, X., 2012. Sp1 is involved in regulation of cystathionine gamma-lyase gene expression and biological function by PI3K/Akt pathway in human hepatocellular carcinoma cell lines. Cell. Signal. 24, 1229–1240.
Yoshioka, Y., Ly, L.L., Yamaguchi, M., 2012. Transcription factor NF-Y is involved in differentiation of R7 photoreceptor cell in Drosophila. Biol. Open 1, 19–29.

Yu, I.T., Park, J.-Y., Kim, S.H., Lee, J.-s., Kim, Y.-S., Son, H., 2009. Valproic acid promotes neuronal differentiation by induction of proneural factors in association with H4 acetylation. Neuropharmacology 56, 473–480.
Zhang, F., Zhang, Z., Kong, D., Zhang, X., Chen, L., Zhu, X., Lu, Y., Zheng, S., 2014. Tetramethylpyrazine reduces glucose and insulin-induced activation of hepatic stellate cells by inhibiting insulin receptor-mediated PI3K/AKT and ERK pathways. Mol. Cell. Endocrinol. 382, 197–204.
Ziemka-Nalecz, M., Zalewska, T., 2012. Endogenous neurogenesis induced by ischemic brain injury or neurodegenerative diseases in adults. Acta Neurobiol. Exp. 72, 309–324.